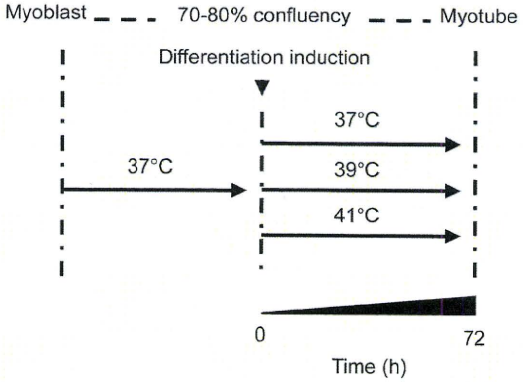

Fig. 1. Heat stress protocols. Cells were seeded in growth medium and incubated at 37°C. When they reached 70–80% confluency, the medium was changed to the differentiation-induction medium. At the same time, the culture temperature was set to 37, 39, or 41°C for 24–72 h.

ersham, UK). The membrane was then blocked in PBS containing 3% skim milk for 1 h and incubated with an appropriately diluted primary antibody and then for 1 h with a horseradish peroxidase-labeled secondary antibody. The immunoreactive bands were detected using an enhanced chemiluminescence kit (Amersham International). The chemiluminescent signal on the membrane was scanned using ChemiDoc XRS, Quantity One quantitation software (Bio-Rad). The band intensity was quantified using NIH Image. The housekeeping protein β-actin was used as an internal loading control for Western blot analysis.

Reverse Transcription-Polymerase Chain Reaction

Total mRNA from HSMM cells was isolated using RNeasy (Qiagen, Valencia, CA). After DNase treatment, cDNAs were obtained by reverse transcription of 2 μg of total RNA (Ready-to-Go T-primed first-strand kit; Amersham Biosciences, Piscataway, NJ). The primer sequences are listed in Table 1 (3, 6, 9, 18, 23, 50). The level of mRNA expression was determined by quantitative real-time reverse transcription-polymerase chain reaction (RT-PCR) in a fluorescent temperature cycler (ABI Prism 7000; Applied Biosystems, Darmstadt, Germany). The housekeeping gene β-actin was used as a control template for normalizing relative change of each mRNA in RT-PCR. Samples were incubated in the ABI Prism 7000 for an initial denaturation at 95°C for 10 min. Next, 40 PCR cycles were performed under the following conditions: 95°C for 15 s and 60°C for 1 min. SYBR green fluorescence (Power SYBR green PCR master mix; Applied Biosystems) emissions were determined after each cycle, and the synthesis of each gene mRNA was quantified using the ABI Prism 7000 SDS software (Applied Biosystems). The PCR was performed in triplicate.

Immunofluorescence

For immunofluorescent staining, cells incubated in petri dishes containing collagen type I-coated cover glasses at 37, 39, and 41°C for 24–72 h were washed with warm PBS at 37°C and fixed by incubation at room temperature in prewarmed (at 37°C) FME (4% formaldehyde, 2 mM $MgCl_2$, and 5 mM EGTA in PBS) for 10 min. Cells were washed three times with PBS and permeabilized with FME containing 0.3% Triton X-100 (FMET) for 10 min at room temperature. FMET-fixed cells were washed three times with PBS and kept in PBS containing 1% BSA and 0.02% sodium azide. Cells were immuno-

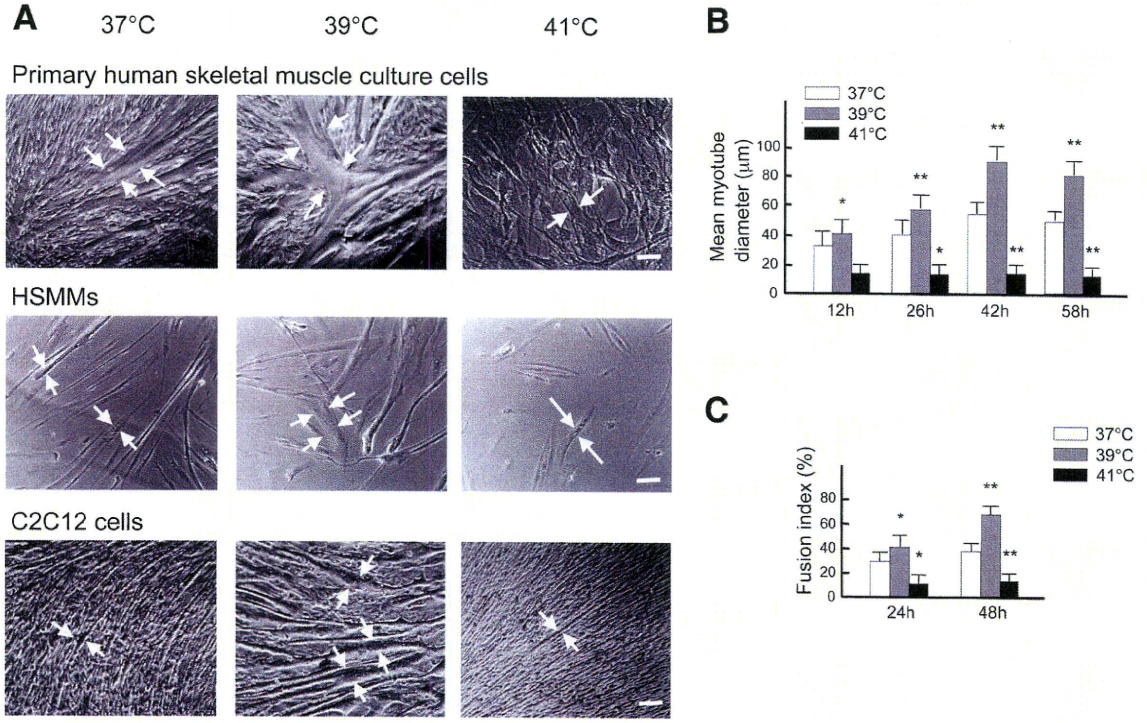

Fig. 2. Morphological changes of human and C2C12 myotubes after exposure to heat stress. *A*: representative images of myotubes in primary human skeletal muscle culture after 72-h exposure to heat stress, human skeletal muscle myoblasts (HSMMs) after 48-h exposure to heat stress, and C2C12 myotubes after 72-h exposure to heat stress. Arrows indicate edges of myotubes. Bars, 80 μm. *B*: changes in myotube diameter formed by C2C12 cells after exposure to heat stress. Each column shows the mean ± SD of 210 myotubes from 3 independent cultures. *C*: changes of fusion index of C2C12 cells after exposure to heat stress. Each column shows the mean ± SD of 3 independent cultures. ; $*P < 0.05$; $**P < 0.01$ compared with control (37°C).

histochemically stained with an appropriately diluted primary antibody and then for 1 h with a fluorescence-conjugated secondary antibody. The slides were then rinsed with PBS and mounting using 4,6-diamidino-2-phenylindole (DAPI). All photographs were viewed in a Nikon Eclipse TE 300 inverted microscope (Tokyo, Japan) and recorded with a digital camera (model 4742-95; Hamamatsu Photonics, Hamamatsu, Japan). Photographs were edited using Photoshop software (Adobe Photoshop version 7.0).

Measurement of Myotube Diameter and Fusion Index of C2C12 Cells

For each temperature condition, 7 different photomicrograph fields were randomly chosen from 3 independent cultures, and the width of the 10 largest myotubes in each field was measured. Mean values constituted a measure of 210 myotubes for each condition. The fusion index was defined as the ratio of the number of DAPI-stained nuclei in myotubes with three or more nuclei to the total number of DAPI-stained nuclei in each field. This percentage was determined by counting 1,000 nuclei per dish on three independent cultures for each condition.

Statistical Analysis

Data are means ± SD. Statistical significance ($P < 0.05$) between control cells incubated at 37°C and heat-stressed cells incubated at 39 or 41°C was determined by a one-way ANOVA followed by a Dunnett post hoc test.

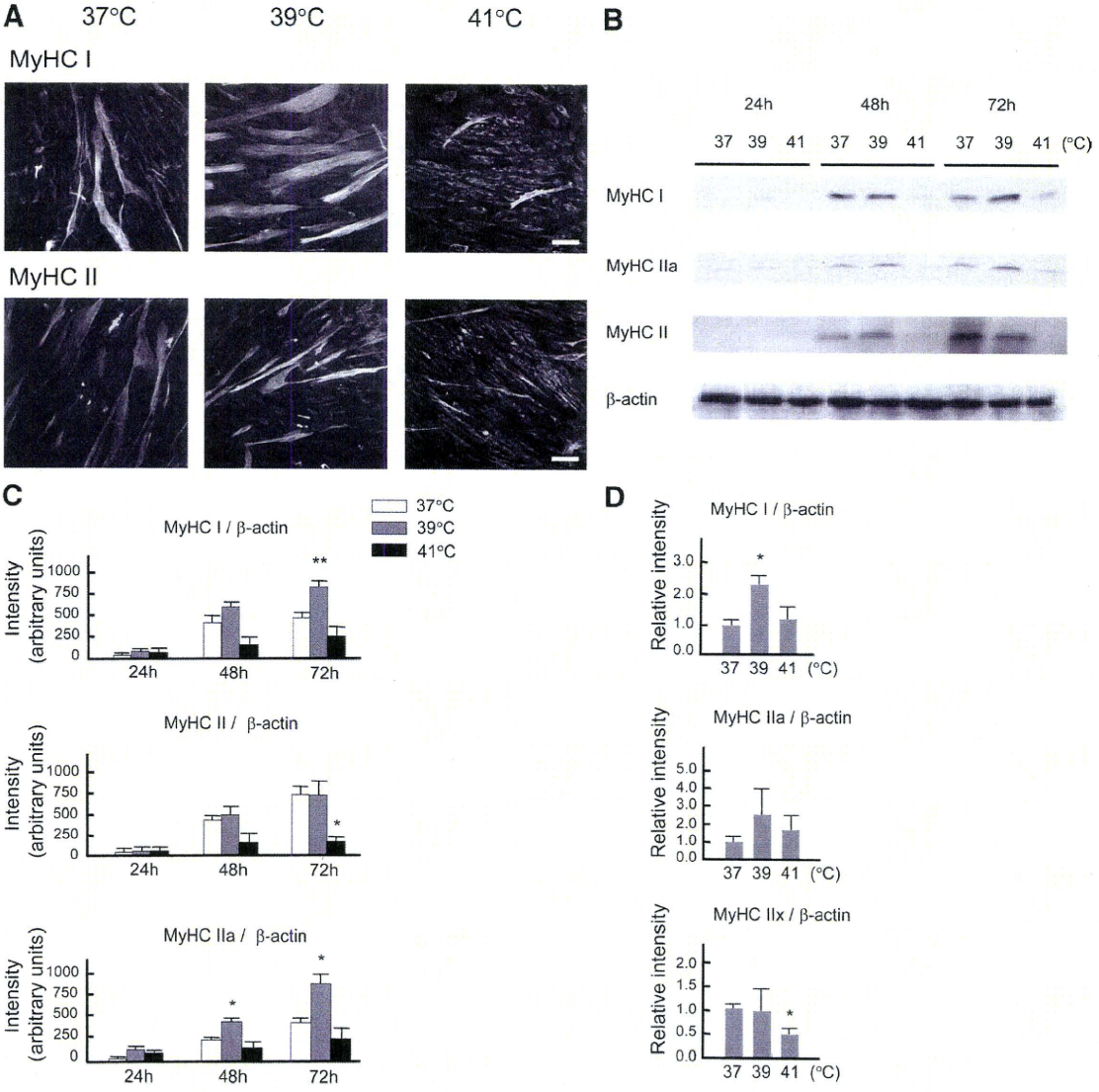

Fig. 3. Changes of myosin heavy chain (MyHC) isoform expression after heat stress treatment of HSMMs. *A*: representative fluorescent images of HSMMs after 72-h exposure to heat stress. MyHC types I and II were detected by immunofluorescence with the use of monoclonal antibodies against MyHC I (clone NOQ7.5.4D) and MyHC II (clone MY32) and secondary rhodamine-conjugated antibody. Bars, 80 μm. *B* and *C*: after exposure of HSMMs to heat stress for 24, 48, and 72 h, cells were harvested and subjected to Western blot analysis with antibodies against MyHC I (clone NOQ7.5.4D), II (clone MY32), and IIa (clone A4.74). MyHC II antibody recognized all the MyHC II isoforms. MyHC isoform expression was normalized to that of β-actin. Data show intensities relative to control (37°C). Data are means ± SD from 3 independent experiments with HSMMs from 3 different donors. *D*: after exposure of HSMMs to heat stress for 72 h, HSMMs were harvested. Total RNA was extracted and reverse transcribed. cDNA levels of MyHC isoform mRNAs in HSMMs were determined by RT-PCR and normalized to β-actin cDNA levels. Data show intensities relative to intensities of control (37°C). Data are means ± SD from 3 independent experiments with HSMMs from 3 different donors. $*P < 0.05$; $**P < 0.01$ compared with control (37°C).

RESULTS

Heat Stress Affects Myotube Formation

To investigate the direct effects of heat stress on myotube formation of cultured mammalian myoblasts, we incubated the cells at various temperatures in vitro, as shown in Fig. 1. Primary human skeletal muscle culture cells were exposed to various temperatures for 72 h. Myotubes incubated at 39°C showed an increased diameter compared with the control cells incubated at 37°C. The myotubes incubated at 41°C were poorly formed (Fig. 2*A*). To minimize the effects of contaminating fibroblasts in primary human skeletal muscle culture cells, we investigated whether a similar phenomenon (myotube enlargement) was observed in HSMMs. The results were consistent with that of the primary culture, with increased diameter when incubated at 39°C (Fig. 2*A*).

To test whether the phenomenon described above was also relevant to muscle cells of mice, we used C2C12 cells, which are of mice origin. As shown in Fig. 2, *A* and *B*, the diameter of the myotubes increased significantly after exposure to 39°C compared with the control cultures at 37°C; interestingly, there was no change in the diameter of the myotubes at 41°C.

Myotubes are formed by the fusion of singly nucleated myoblasts by differentiation-inducing stimuli. Hence, the enlargement of myotubes incubated at 39°C could be due to differences in the fusion process of myoblasts. To test this possibility, we measured the fusion index of C2C12 cells incubated at different temperatures. Compared with the control culture at 37°C, the fusion index was significantly increased at 39°C after 24 and 48 h of incubation, whereas the fusion index was significantly decreased at 41°C (Fig. 2*C*).

To identify temperature-dependent expression of HSPs after continuous heat stress, we analyzed the protein expression levels of a representative HSP (HSP70) by Western blot analysis of HSMMs extracts. In cells exposed to heat stress for 72 h, the protein level of HSP70 increased 2.7-fold at 39°C and 7.3-fold at 41°C compared with 37°C control (data not shown).

Heat exposure alters levels of MyHC isoforms in HSMMs and C2C12 cells

Since the function of skeletal muscle cells is highly linked to their structure, it is possible that the structural change, i.e., increased myotube diameter as described above, is accompanied by some functional changes in skeletal muscle cells. To test this possibility, we examined possible changes in MyHC isoforms in cells exposed to heat stress. Figure 3, *A* and *B*, shows representative immunostaining of HSMMs. The MyHC was targeted by either a primary antibody specific for MyHC I (NOQ7.5.4D) or an antibody specific for MyHC II (MY-32) (Fig. 3*A*). MY-32 recognized all MyHC II isoforms. These experiments indicated that HSMMs expressed both MyHC I and II. After exposure to heat stress for 72 h, HSMM myotubes expressing MyHC I at 39°C were larger in size compared with myotubes that were not heat-stressed. In contrast, HSMM myotubes expressing MyHC II at 39°C were of the same size compared with myotubes exposed to 37°C. The myotubes incubated at 41°C showed weak staining for both MyHC I and II.

In adult humans, there are three major MyHC isoforms (MyHC I and two subtypes of MyHC II, IIa and IIx) (12). Expression of MyHC I and II isoforms in HSMMs was confirmed by Western blot analysis and RT-PCR. We used β-actin as an internal control. There were no significant changes in the protein and mRNA levels of β-actin after heat stress in HSMMs (data not shown). To examine the protein levels of MyHC isoforms in HSMMs, we used MyHC I (NOQ7.5.4D), II (MY-32), and IIa (A4.74) (22) antibodies. As shown in Fig. 3, *B* and *C*, in HSMMs exposed to heat stress at 39°C, the protein levels of MyHC I increased after 72 h of incubation (1.6-fold, $P < 0.01$), whereas MyHC I protein levels were unaffected by heat stress at 41°C, compared with the control culture at 37°C. MyHC II antibody recognized both MyHC II isoforms. The total protein level of MyHC II did not change at 39°C after heat exposure but decreased at 41°C after 72 h ($P < 0.05$) compared with the 37°C control. In contrast, in cells exposed to heat stress at 39°C for 48 and 72 h, 1.8-fold ($P < 0.05$) and 2.1-fold increases ($P < 0.05$), respectively, were found in the levels of MyHC IIa protein compared with the 37°C control. Those results implied that MyHC IIx expression decreased after exposure to heat stress at 39°C. We also

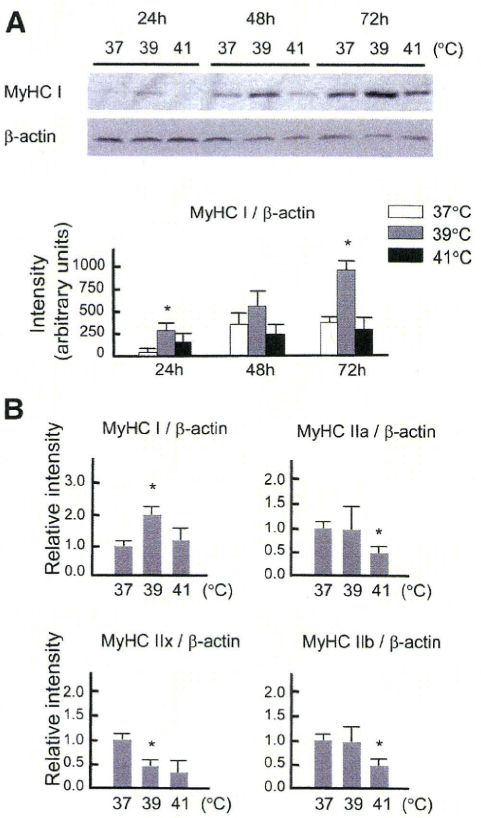

Fig. 4. Changes of MyHC isoform expression after heat stress treatment of C2C12 cells. *A*: after exposure of C2C12 cells to heat stress for 24, 48, and 72 h, cells were harvested and subjected to Western blot analysis with an antibody against MyHC type I. MyHC type I expression was normalized to β-actin. Data show intensities relative to control (37°C). Data are means ± SD from 3 independent cell cultures. *B*: after exposure of C2C12 cells to heat stress for 72 h, C2C12 cells were harvested. Total RNA was extracted and reverse transcribed. cDNA levels of MyHC isoform mRNAs in C2C12 cells were determined by RT-PCR and normalized to β-actin cDNA levels. Data show intensities relative to intensities of control (37°C). Data are means ± SD from 3 independent cell cultures. $*P < 0.05$; $**P < 0.01$ compared with control (37°C).

examined corresponding changes in the mRNA levels of MyHC isoforms in HSMMs. As shown in Fig. 3*D*, in HSMMs exposed to heat stress at 39°C for 72 h, the mRNA levels of MyHC I increased 2.3-fold compared with cells that were not heat-stressed ($P < 0.05$), whereas the mRNA levels of MyHC IIa tended to increase when cells were exposed to 39°C ($P = 0.23$). In contrast, the mRNA levels of MyHC IIx in cells exposed to 41°C decreased 47% compared with cells that were not heat-stressed ($P < 0.05$). These data indicated that incubation of cells at 39°C induced differentiation, leading to a fast-to-slow fiber-type shift in HSMMs.

In small mammals, there are four major MyHC isoforms in skeletal muscle fibers: MyHC I and three subtypes of MyHC II, IIa, IIx, and IIb (39). Expression of MyHC I and II isoforms in C2C12 cells was confirmed by Western blot analysis and RT-PCR. We used β-actin as an internal control. There were no significant changes in the protein and mRNA levels of β-actin after heat stress in C2C12 cells (data not shown). To examine the protein expression of MyHC I in C2C12 cells, we used an antibody targeted against MyHC I (NOQ7.5.4D). In cells exposed to 39°C, the protein level of MyHC I increased after 24 (4.8-fold, $P < 0.05$) and 72 h (2.4-fold, $P < 0.05$) of incubation compared with cells that were not heat-stressed (Fig. 4*A*). We examined changes in expression of MyHC I and II isoforms in C2C12 cells by using RT-PCR. As shown in Fig. 4*B*, in C2C12 cells exposed to heat stress at 39°C for 72 h, the mRNA levels of MyHC I increased 2.0-fold compared with cells that were not heat-stressed ($P < 0.05$), whereas the mRNA levels of MyHC IIx in cells exposed to 39°C decreased 45% compared with cells that were not heat-stressed ($P < 0.05$). These data indicated that incubation of cells at 39°C induced differentiation, leading to a fast-to-slow fiber-type shift in C2C12 cells.

Heat Exposure Alters Levels of MRFs in HSMMs and C2C12 Cells

MRFs, which include MyoD and myogenin, are expressed in skeletal muscle, with each MRF playing a crucial role in muscle cell specification and differentiation (44). MyoD mRNA was shown to be most prevalent in fast glycolytic muscles, whereas myogenin mRNA was shown to be most prevalent in slow oxidative muscles (15). To test the possible involvement of MRFs in the myotube enlargement and the fiber-type shift in heat-stressed cells, we next addressed the protein levels of MyoD and myogenin in both types of cells after a 72-h exposure to heat stress. The level of myogenin was enhanced in the 39°C culture ($P < 0.05$) relative to that at 37°C, but no significant change in the levels of MyoD was detected after heat stress in HSMMs (Fig. 5*A*). We further tested whether there were any changes in the levels of MyoD and myogenin in C2C12 cells after heat stress. In cells exposed to heat stress for 72 h, the protein levels of MyoD decreased at 39 ($P < 0.05$) and 41°C ($P < 0.01$), whereas the protein levels of myogenin increased at 39°C ($P < 0.01$), compared with cells that were not exposed to heat stress (Fig. 5*B*). Figure 5*C* shows representative immunostaining for myogenin in C2C12 cells. Large myotubes at 39°C contained more myogenin-positive nuclei than did myotubes at 37°C. These data suggested that incubation of cells at 39°C induced myogenin expression, which enhanced myoblast fusion.

Heat Exposure Alters PGC-1α Protein Expression in HSMMs and C2C12 Cells

PGC-1α is one of the factors regulating muscle fiber-type determination (21). To determine any changes in expression of PGC-1α after exposure of cells to heat stress, we examined the protein level of PGC-1α in C2C12 cells after heat stress. In cells exposed to 39°C, the protein level of PGC-1α increased after 48 ($P < 0.05$) and 72 h ($P < 0.01$) of incubation compared with cells that were not heat-stressed (Fig. 6*A*). When we examined the protein level of PGC-1α in HSMMs by Western blot analysis, it could not be detected at any point in time (24, 48, and 72 h). Thus we determined PGC-1α expression in HSMMs by RT-PCR. After heat stress for 24 h, the mRNA level of PGC-1α was enhanced in the 39°C culture

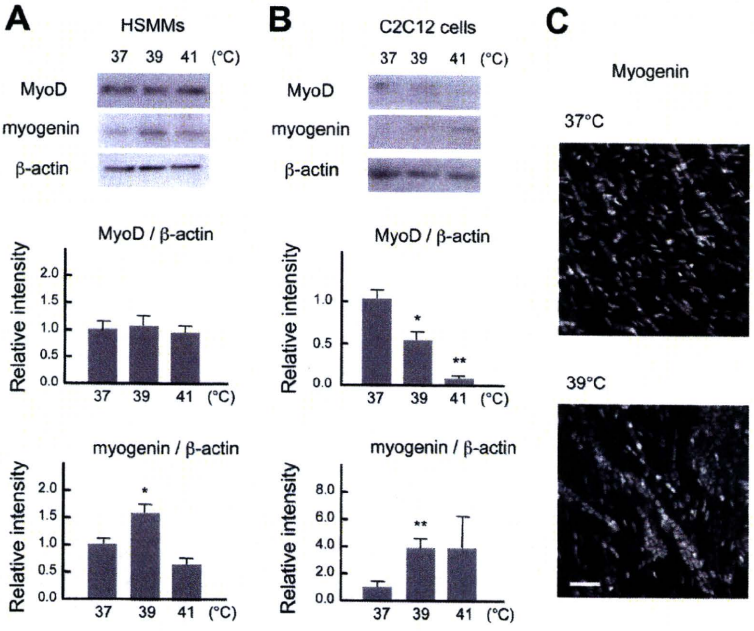

Fig. 5. Changes in the levels of MyoD and myogenin after heat stress treatment of HSMMs and C2C12 cells. *A* and *B*: After exposure to heat stress for 72 h, cells were harvested and subjected to Western blot analysis with antibodies against MyoD and myogenin. Expression of MyoD and myogenin was normalized to β-actin. Data show intensities relative to intensities of control (37°C). Data are means ± SD from 3 independent experiments with HSMMs from 3 different donors (*A*) or 3 C2C12 cell cultures (*B*). *$P < 0.05$; **$P < 0.01$ compared with control (37°C). *C*: representative fluorescent images of C2C12 cells after 72-h exposure to heat stress. Myogenin was detected by immunofluorescence with the use of monoclonal anti-myogenin antibody (F5D) and secondary rhodamine-conjugated antibody. Bars, 80 μm.

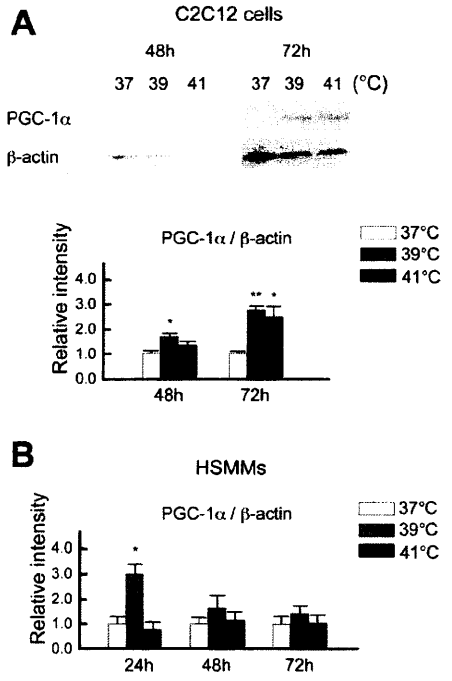

Fig. 6. Changes of the levels of peroxisome proliferator-activated receptor-γ coactivator-1α (PGC-1α) after heat stress in C2C12 cells and HSMMs. *A*: after exposure of C2C12 cells to heat stress for 48 and 72 h, cells were harvested and subjected to Western blot analysis with an antibody against PGC-1α. PGC-1α expression was normalized to β-actin. Data express intensities relative to control (37°C). Data are means ± SD from 3 independent cell cultures. *B*: after exposure of HSMMs to heat stress for 24, 48, and 72 h, HSMMs were harvested. Total RNA was extracted and reverse transcribed. cDNA levels of MyHC isoform mRNAs in HSMMs were determined by RT-PCR and normalized to β-actin cDNA levels. Data show intensities relative to control (37°C). Data are means ± SD from 3 independent experiments with HSMMs from 3 different donors. $*P < 0.05$; $**P < 0.01$ compared with each control (37°C).

($P < 0.05$) relative to that at 37°C, but no significant change in the mRNA levels of PGC-1α was detected after heat stress for 48 and 72 h in HSMMs (Fig. 6*B*).

Several studies have shown that MAPKs are involved in the determination of muscle fiber type phenotypes (27, 31). It is possible that heat stress affected the phosphorylation of ERK1/2 or p38 MAPK. ERK1/2 is activated by short- and long-term low-frequency electrical stimulation, which involved fast-to-slow fiber-type conversion (2, 31). Thus we next measured the phosphorylation states of ERK1/2 and p38 MAPK in HSMMs and C2C12 cells after heat stress for 1, 24, and 48 h. The relative amounts of phosphorylated forms of both ERK1/2 and p38 MAPK did not change at any point in time in either type of cells (data not shown).

DISCUSSION

We defined incubation at 39°C as continuous mild heat stress (CMHS) and 41°C as continuous severe heat stress (CSHS). Our analysis revealed that CMHS enhanced myotube diameter of primary human skeletal muscle culture cells, HSMMs, and C2C12 cells. In contrast, during CSHS, myotubes were poorly formed. In HSMMs and C2C12 cells exposed to CMHS, the mRNA and protein levels of MyHC type I was increased compared with the control cultures. The mRNA level of MyHC IIx was unaltered in HSMMs and decreased in C2C12 cells compared with cells that were not exposed to heat stress. These results indicate that CMHS induced the differentiation of the cells, causing a fast-to-slow fiber-type shift in C2C12 cells and HSMMs. Our results also showed upregulated myogenin expression after CMHS. We next examined upstream signals that might be responsible for the fiber-type shift. CMHS enhanced mRNA and protein levels of PGC-1α in HSMMs and C2C12 cells.

The effects of heat stress on cellular function are pleiotropic. These include denaturation and disaggregation of proteins, cytoskeletal disruption, cell cycle inhibition, and changes in membrane permeability (20). Heat stress induces HSP70, which plays a role in maintaining protein homeostasis, a fine balance among protein synthesis, protein degradation, and protein refolding (38, 51). In addition, detection of HSPs is an indication of the formation of denatured protein and the presence of thermal damage (20). In our study, the levels of HSP70 were upregulated with increased temperature after heat stress. Since myogenic differentiation was not inhibited during CMHS, the amount of protein denaturation may be low. In contrast, CSHS inhibited myotube formation. CSHS might increase the amount of denatured and aggregated proteins and disrupt protein homeostasis, which might in turn lead to intracellular dysfunction.

The fast-to-slow shift in MyHC isoform expression can be induced under several conditions. Strength training led to a shift in MyHC isoform composition from MyHC IIx to IIa in human triceps brachii (23). Chronic low-frequency electrical stimulation (CLFS) increases the expression of MyHC I or IIa, whereas it decreases that of MyHC IIx or IIb in human and rat tibialis anterior (26, 47). So far, changes of MyHC following heat stress have not been reported. Our study is the first to report that CMHS induced differentiation and a fast-to-slow fiber-type shift of myoblasts in two different species. These observations might be a general characteristic of mammalian myoblasts.

Several signaling pathways regulate skeletal muscle fiber-type shift. Murgia et al. (31) suggested that the Ras-ERK pathway was required for reestablishment of the slow fiber program in a model simulating nerve impulse activity. p38 MAPK has been reported to control MyHC IIx promoter activity in myotubes (27). Our study demonstrated that CMHS did not enhance the activity of either ERK1/2 or p38 MAPK. Another investigator suggested that the ERK1/2 pathway played an important role in the maintenance of fast-twitch fiber phenotype (41). So far, the role of MAPK signaling cascades in modulating muscle fiber type remains unclear.

Transgenic expression of PGC-1α in fast-twitch glycolytic muscles promotes mitochondrial biogenesis and oxidative metabolism and transforms the type IIb muscle fibers into a more oxidative phenotype (21). Therefore, PGC-1α might be the principal factor regulating muscle fiber-type determination. AMP-activated protein kinase (AMPK), calcineurin, CaMK, and p38 MAPK pathways have been implicated in the regulation of PGC-1α expression and activity (8). Since the activation of p38 MAPK did not change, the expression of PGC-1α induced by CMHS in the present study might be attributable to other pathways. Calcium is thought to be involved in the upstream signaling of PGC-1α for several reasons. Calcium activates calcineurin and CaMK, which regulate the expression

of PGC-1α (8, 48). Kubis et al. (17) reported that a modest but sustained rise in intracellular free Ca^{2+} concentration ($[Ca^{2+}]_i$) caused by low concentrations of the Ca^{2+} ionophore A-23187 in the culture medium induced fast-to-slow fiber-type conversion in rabbit primary skeletal muscle cells. With regard to heat stress and Ca^{2+} homeostasis, heat stress is known to increase $[Ca^{2+}]_i$ (5, 28). Recent evidence suggests that exposure of mammalian skeletal muscle to temperatures in the range of 40–43°C for 30 min reduced the ability of the sarcoplasmic reticulum to accumulate Ca^{2+} (46). Accordingly, CMHS may induce changes in Ca^{2+} homeostasis, which could lead to the fiber-type shift through the PGC-1α pathway in myoblasts.

In the present study, CMHS enhanced the level of expression of myogenin protein, whereas there was no increase in the level of MyoD. CMHS enhanced myoblast fusion and myotube diameter of C2C12 cells and HSMMs. Myogenin is required to initiate terminal differentiation and fusion (1, 25). These results indicated that myogenin played a role in CMHS-enhanced myogenic differentiation. It has been reported that MyoD is prevalent in fast-twitch muscles and myogenin in slow-twitch muscles (15). Several lines of evidence have implicated myogenin in the fast-to-slow fiber-type shift (7, 15, 26, 37, 47). In cultured myotubes, a moderate increase in $[Ca^{2+}]_i$ induced a fast-to-slow fiber-type shift and enhanced the protein expression level of myogenin but not other myogenic factors (45). In the fast-twitch muscle of hypothyroid rats, shifting to a slow direction by CLFS increased the expression of myogenin with unaltered MyoD levels (37). Hughes et al. (14) reported that the overexpression of myogenin in skeletal muscles of transgenic mice influenced the activity of metabolic enzymes, inducing a shift from glycolytic metabolism to oxidative metabolism. In their study, no change in fiber type-specific MyHC isoform expression was observed. Furthermore, Schluter and Fitts (40) reported that oxidative enzyme activity and MyHC type were independently regulated in rat skeletal muscle. Thus it appears that myogenin plays a role in metabolic adaptation to a fast-to-slow fiber-type shift, although no study has demonstrated the link between myogenin expression and mild changes in temperature.

The results of this study showed that CMHS increased the fusion index, myotube diameter, and fast-to-slow fiber-type shift, whereas CSHS did not promote myotube formation. The beneficial effect of low doses of a stressful agent, which is otherwise toxic at high doses, is known as hormesis (24). Although local hyperthermia is used to promote blood flow and enhance healing after muscle injuries (19), the mechanism by which this occurs has not been fully elucidated. During hyperthermia, temperature in skeletal muscle ranges from 36 to 44°C (4, 19). On skeletal muscle injury, satellite cells are released and activated to become myoblasts, which eventually differentiate into myotubes and mature muscle fibers (13). We observed the effects of temperature on the in vitro differentiation of myoblasts and have elucidated a possible mechanism of heat stress. We postulate that local hyperthermia increases muscle temperature and thereby promotes myogenic differentiation and fast-to-slow muscle fiber-type shift in vivo.

There is increasing evidence suggesting that mitochondrial dysfunction in skeletal muscle is involved in insulin resistance and type 2 diabetes (16). PGC-1α promotes mitochondrial biogenesis and slow fiber formation in skeletal muscle (21). Two studies have reported that decreases in the amount of PGC-1α in skeletal muscle are associated with human type 2 diabetes and an increased risk of developing type 2 diabetes (29, 34). Taking these findings together, PGC-1α appears to play a role in disorders such as insulin resistance and diabetes. Also, several lines of evidence demonstrate that both short-term exercise and endurance training activate PGC-1α expression in skeletal muscle (8, 36). Pilegaard et al. (36) reported that exercise induces a dramatic transient increase in PGC-1α transcription and mRNA content, peaking within 2 h after exercise in human skeletal muscle. Our observations of PGC-1α mRNA expression in HSMMs were similar to that reported by Pilegaard (36). It is possible that a mild increase in temperature due to exercise causes PGC-1α expression. Further studies of CMHS should provide insight into prevention of diseases involving mitochondrial dysfunction and identify factors that induce PGC-1α following exercise.

ACKNOWLEDGMENTS

We thank Dr. Kiyoshi Kikumoto for providing human skeletal muscle samples. We also thank Drs. Takashi Sakurai and Shunichiro Kubota for generous support of our research. We are grateful to Dr. Ryoichi Matsuda for kindly providing antibodies.

REFERENCES

1. **Andres V, Walsh K.** Myogenin expression, cell cycle withdrawal, and phenotypic differentiation are temporally separable events that precede cell fusion upon myogenesis. *J Cell Biol* 132: 657–666, 1996.
2. **Aronson D, Dufresne SD, Goodyear LJ.** Contractile activity stimulates the c-Jun NH_2-terminal kinase pathway in rat skeletal muscle. *J Biol Chem* 272: 25636–25640, 1997.
3. **Balagopal P, Olney R, Darmaun D, Mougey E, Dokler M, Sieck G, Hammond D.** Oxandrolone enhances skeletal muscle myosin synthesis and alters global gene expression profile in Duchenne muscular dystrophy. *Am J Physiol Endocrinol Metab* 290: E530–E539, 2006.
4. **Borrell RM, Parker R, Henley EJ, Masley D, Repinecz M.** Comparison of in vivo temperatures produced by hydrotherapy, paraffin wax treatment, and Fluidotherapy. *Phys Ther* 60: 1273–1276, 1980.
5. **Calderwood SK, Stevenson MA, Hahn GM.** Effects of heat on cell calcium and inositol lipid metabolism. *Radiat Res* 113: 414–425, 1988.
6. **Casas F, Pessemesse L, Grandemange S, Seyer P, Gueguen N, Baris O, Lepourry L, Cabello G, Wrutniak-Cabello C.** Overexpression of the mitochondrial T3 receptor p43 induces a shift in skeletal muscle fiber types. *PLoS One* 3: e2501, 2008.
7. **Ekmark M, Gronevik E, Schjerling P, Gundersen K.** Myogenin induces higher oxidative capacity in pre-existing mouse muscle fibres after somatic DNA transfer. *J Physiol* 548: 259–269, 2003.
8. **Finck BN, Kelly DP.** PGC-1 coactivators: inducible regulators of energy metabolism in health and disease. *J Clin Invest* 116: 615–622, 2006.
9. **Frederiksen CM, Hojlund K, Hansen L, Oakeley EJ, Hemmings B, Abdallah BM, Brusgaard K, Beck-Nielsen H, Gaster M.** Transcriptional profiling of myotubes from patients with type 2 diabetes: no evidence for a primary defect in oxidative phosphorylation genes. *Diabetologia* 51: 2068–2077, 2008.
10. **Gaster M, Beck-Nielsen H, Schroder HD.** Proliferation conditions for human satellite cells. The fractional content of satellite cells. *APMIS* 109: 726–734, 2001.
11. **Hanson DF.** Fever, temperature, and the immune response. *Ann NY Acad Sci* 813: 453–464, 1997.
12. **Hilber K, Galler S, Gohlsch B, Pette D.** Kinetic properties of myosin heavy chain isoforms in single fibers from human skeletal muscle. *FEBS Lett* 455: 267–270, 1999.
13. **Huard J, Li Y, Fu FH.** Muscle injuries and repair: current trends in research. *J Bone Joint Surg Am* 84-A: 822–832, 2002.
14. **Hughes SM, Chi MM, Lowry OH, Gundersen K.** Myogenin induces a shift of enzyme activity from glycolytic to oxidative metabolism in muscles of transgenic mice. *J Cell Biol* 145: 633–642, 1999.
15. **Hughes SM, Taylor JM, Tapscott SJ, Gurley CM, Carter WJ, Peterson CA.** Selective accumulation of MyoD and myogenin mRNAs in fast and slow adult skeletal muscle is controlled by innervation and hormones. *Development* 118: 1137–1147, 1993.

16. **Kelley DE, He J, Menshikova EV, Ritov VB.** Dysfunction of mitochondria in human skeletal muscle in type 2 diabetes. *Diabetes* 51: 2944–2950, 2002.
17. **Kubis HP, Haller EA, Wetzel P, Gros G.** Adult fast myosin pattern and Ca^{2+}-induced slow myosin pattern in primary skeletal muscle culture. *Proc Natl Acad Sci USA* 94: 4205–4210, 1997.
18. **Lamba DA, Karl MO, Ware CB, Reh TA.** Efficient generation of retinal progenitor cells from human embryonic stem cells. *Proc Natl Acad Sci USA* 103: 12769–12774, 2006.
19. **Lehmann JF, de Lateur BJ.** Diathermy and superficial heat, laser and cold therapy. In: *Krusen's Handbook of Physical Medicine and Rehabilitation*, edited by Kottke FJ and Lehmann JF. Philadelphia, PA: Saunders, 1990. p. 283–435.
20. **Lepock JR.** Cellular effects of hyperthermia: relevance to the minimum dose for thermal damage. *Int J Hyperthermia* 19: 252–266, 2003.
21. **Lin J, Wu H, Tarr PT, Zhang CY, Wu Z, Boss O, Michael LF, Puigserver P, Isotani E, Olson EN, Lowell BB, Bassel-Duby R, Spiegelman BM.** Transcriptional co-activator PGC-1 alpha drives the formation of slow-twitch muscle fibres. *Nature* 418: 797–801, 2002.
22. **Liu JX, Thornell LE, Pedrosa-Domellof F.** Muscle spindles in the deep muscles of the human neck: a morphological and immunocytochemical study. *J Histochem Cytochem* 51: 175–186, 2003.
23. **Liu Y, Schlumberger A, Wirth K, Schmidtbleicher D, Steinacker JM.** Different effects on human skeletal myosin heavy chain isoform expression: strength vs. combination training. *J Appl Physiol* 94: 2282–2288, 2003.
24. **Luckey T.** *Hormesis with Ionizing Radiation.* Boca Raton, FL: CRC, 1980.
25. **Ludolph DC, Konieczny SF.** Transcription factor families: muscling in on the myogenic program. *FASEB J* 9: 1595–1604, 1995.
26. **Martins KJ, Gordon T, Pette D, Dixon WT, Foxcroft GR, Maclean IM, Putman CT.** Effect of satellite cell ablation on low-frequency-stimulated fast-to-slow fibre-type transitions in rat skeletal muscle. *J Physiol* 572: 281–294, 2006.
27. **Meissner JD, Chang KC, Kubis HP, Nebreda AR, Gros G, Scheibe RJ.** The p38alpha/beta mitogen-activated protein kinases mediate recruitment of CREB-binding protein to preserve fast myosin heavy chain IId/x gene activity in myotubes. *J Biol Chem* 282: 7265–7275, 2007.
28. **Mikkelsen RB, Reinlib L, Donowitz M, Zahniser D.** Hyperthermia effects on cytosolic $[Ca^{2+}]$: analysis at the single cell level by digitized imaging microscopy and cell survival. *Cancer Res* 51: 359–364, 1991.
29. **Mootha VK, Lindgren CM, Eriksson KF, Subramanian A, Sihag S, Lehar J, Puigserver P, Carlsson E, Ridderstrale M, Laurila E, Houstis N, Daly MJ, Patterson N, Mesirov JP, Golub TR, Tamayo P, Spiegelman B, Lander ES, Hirschhorn JN, Altshuler D, Groop LC.** PGC-1alpha-responsive genes involved in oxidative phosphorylation are coordinately downregulated in human diabetes. *Nat Genet* 34: 267–273, 2003.
30. **Moyer HR, Delman KA.** The role of hyperthermia in optimizing tumor response to regional therapy. *Int J Hyperthermia* 24: 251–261, 2008.
31. **Murgia M, Serrano AL, Calabria E, Pallafacchina G, Lomo T, Schiaffino S.** Ras is involved in nerve-activity-dependent regulation of muscle genes. *Nat Cell Biol* 2: 142–147, 2000.
32. **Naya FJ, Mercer B, Shelton J, Richardson JA, Williams RS, Olson EN.** Stimulation of slow skeletal muscle fiber gene expression by calcineurin in vivo. *J Biol Chem* 275: 4545–4548, 2000.
33. **Park HG, Han SI, Oh SY, Kang HS.** Cellular responses to mild heat stress. *Cell Mol Life Sci* 62: 10–23, 2005.
34. **Patti ME, Butte AJ, Crunkhorn S, Cusi K, Berria R, Kashyap S, Miyazaki Y, Kohane I, Costello M, Saccone R, Landaker EJ, Goldfine AB, Mun E, DeFronzo R, Finlayson J, Kahn CR, Mandarino LJ.** Coordinated reduction of genes of oxidative metabolism in humans with insulin resistance and diabetes: potential role of PGC1 and NRF1. *Proc Natl Acad Sci USA* 100: 8466–8471, 2003.
35. **Pette D, Staron RS.** Myosin isoforms, muscle fiber types, and transitions. *Microsc Res Tech* 50: 500–509, 2000.
36. **Pilegaard H, Saltin B, Neufer PD.** Exercise induces transient transcriptional activation of the PGC-1alpha gene in human skeletal muscle. *J Physiol* 546: 851–858, 2003.
37. **Putman CT, Dusterhoft S, Pette D.** Satellite cell proliferation in low frequency-stimulated fast muscle of hypothyroid rat. *Am J Physiol Cell Physiol* 279: C682–C690, 2000.
38. **Rokutan K, Hirakawa T, Teshima S, Nakano Y, Miyoshi M, Kawai T, Konda E, Morinaga H, Nikawa T, Kishi K.** Implications of heat shock/stress proteins for medicine and disease. *J Med Invest* 44: 137–147, 1998.
39. **Schiaffino S, Reggiani C.** Myosin isoforms in mammalian skeletal muscle. *J Appl Physiol* 77: 493–501, 1994.
40. **Schluter JM, Fitts RH.** Shortening velocity and ATPase activity of rat skeletal muscle fibers: effects of endurance exercise training. *Am J Physiol Cell Physiol* 266: C1699–C1713, 1994.
41. **Shi H, Scheffler JM, Pleitner JM, Zeng C, Park S, Hannon KM, Grant AL, Gerrard DE.** Modulation of skeletal muscle fiber type by mitogen-activated protein kinase signaling. *FASEB J* 22: 2990–3000, 2008.
42. **Shui C, Scutt A.** Mild heat shock induces proliferation, alkaline phosphatase activity, and mineralization in human bone marrow stromal cells and Mg-63 cells in vitro. *J Bone Miner Res* 16: 731–741, 2001.
43. **Smith W.** The application of cold and heat in the treatment of athletic injuries. In: *Thermal Agents in Rehabilitation*, edited by Michlovitz SL. Philadelphia, PA: Davis, 1990. p. 245–256.
44. **Tapscott SJ.** The circuitry of a master switch: MyoD and the regulation of skeletal muscle gene transcription. *Development* 132: 2685–2695, 2005.
45. **Thelen MH, Simonides WS, Muller A, van Hardeveld C.** Cross-talk between transcriptional regulation by thyroid hormone and myogenin: new aspects of the Ca^{2+}-dependent expression of the fast-type sarcoplasmic reticulum Ca^{2+}-ATPase. *Biochem J* 329: 131–136, 1998.
46. **van der Poel C, Stephenson DG.** Effects of elevated physiological temperatures on sarcoplasmic reticulum function in mechanically skinned muscle fibers of the rat. *Am J Physiol Cell Physiol* 293: C133–C141, 2007.
47. **Vissing K, Andersen JL, Harridge SD, Sandri C, Hartkopp A, Kjaer M, Schjerling P.** Gene expression of myogenic factors and phenotype-specific markers in electrically stimulated muscle of paraplegics. *J Appl Physiol* 99: 164–172, 2005.
48. **Wu H, Kanatous SB, Thurmond FA, Gallardo T, Isotani E, Bassel-Duby R, Williams RS.** Regulation of mitochondrial biogenesis in skeletal muscle by CaMK. *Science* 296: 349–352, 2002.
49. **Wust P, Gellermann J, Rau B, Loffel J, Speidel A, Stahl H, Riess H, Vogl TJ, Felix R, Schlag PM.** Hyperthermia in the multimodal therapy of advanced rectal carcinomas. *Recent Results Cancer Res* 142: 281–309, 1996.
50. **Xu X, Zhang W, Kone BC.** CREB trans-activates the murine H^+-K^+-ATPase α_2-subunit gene. *Am J Physiol Cell Physiol* 287: C903–C911, 2004.
51. **Yamaguchi T, Arai H, Katayama N, Ishikawa T, Kikumoto K, Atomi Y.** Age-related increase of insoluble, phosphorylated small heat shock proteins in human skeletal muscle. *J Gerontol A Biol Sci Med Sci* 62: 481–489, 2007.

MTOpen

Efficient Generation of Hepatoblasts From Human ES Cells and iPS Cells by Transient Overexpression of Homeobox Gene *HEX*

Mitsuru Inamura[1,2], Kenji Kawabata[2,3], Kazuo Takayama[1,2], Katsuhisa Tashiro[2], Fuminori Sakurai[2], Kazufumi Katayama[1,2], Masashi Toyoda[4], Hidenori Akutsu[4], Yoshitaka Miyagawa[5], Hajime Okita[5], Nobutaka Kiyokawa[5], Akihiro Umezawa[4], Takao Hayakawa[6,7], Miho K Furue[8,9] and Hiroyuki Mizuguchi[1,2]

[1]*Department of Biochemistry and Molecular Biology, Graduate School of Pharmaceutical Sciences, Osaka University, Osaka, Japan;* [2]*Laboratory of Stem Cell Regulation, National Institute of Biomedical Innovation, Osaka, Japan;* [3]*Department of Biomedical Innovation, Graduate School of Pharmaceutical Science, Osaka University, Osaka, Japan;* [4]*Department of Reproductive Biology, National Institute for Child Health and Development, Tokyo, Japan;* [5]*Department of Developmental Biology and Pathology, National Institute for Child Health and Development, Tokyo, Japan;* [6]*Pharmaceutics and Medical Devices Agency, Tokyo, Japan;* [7]*Pharmaceutical Research and Technology Institute, Kinki University, Osaka, Japan;* [8]*JCRB Cell Bank/Laboratory of Cell Culture, Department of Disease Bioresource, National Institute of Biomedical Innovation, Osaka, Japan;* [9]*Laboratory of Cell Processing, Institute for Frontier Medical Sciences, Kyoto University, Kyoto, Japan*

Human embryonic stem cells (ESCs) and induced pluripotent stem cells (iPSCs) have the potential to differentiate into all cell lineages, including hepatocytes, *in vitro*. Induced hepatocytes have a wide range of potential application in biomedical research, drug discovery, and the treatment of liver disease. However, the existing protocols for hepatic differentiation of PSCs are not very efficient. In this study, we developed an efficient method to induce hepatoblasts, which are progenitors of hepatocytes, from human ESCs and iPSCs by overexpression of the *HEX* gene, which is a homeotic gene and also essential for hepatic differentiation, using a HEX-expressing adenovirus (Ad) vector under serum/feeder cell-free chemically defined conditions. Ad-HEX-transduced cells expressed α-fetoprotein (AFP) at day 9 and then expressed albumin (ALB) at day 12. Furthermore, the Ad-HEX-transduced cells derived from human iPSCs also produced several cytochrome P450 (CYP) isozymes, and these P450 isozymes were capable of converting the substrates to metabolites and responding to the chemical stimulation. Our differentiation protocol using Ad vector-mediated transient HEX transduction under chemically defined conditions efficiently generates hepatoblasts from human ESCs and iPSCs. Thus, our methods would be useful for not only drug screening but also therapeutic applications.

Received 18 March 2010; accepted 13 October 2010; published online 23 November 2010. doi:10.1038/mt.2010.241

INTRODUCTION

Human embryonic stem cells (ESCs) and induced pluripotent stem cells (iPSCs) are able to replicate indefinitely and differentiate into most cell types of the body,[1–4] and thereby have the potential to provide an unlimited source of cells for a variety of applications.[5] Hepatocytes are useful cells for biomedical research, regenerative medicine, and drug discovery. They are particularly applicable to drug screenings, such as for the determination of metabolic and toxicological properties of drug compounds in *in vitro* models, because the liver is the main detoxification organ in the body.[6] For these applications, it is necessary to prepare a large number of functional hepatocytes from human ESCs and iPSCs. Many of the existing methods for cell differentiation of human ESCs and iPSCs into hepatocytes employ undefined, serum-containing medium and feeder cells.[7–9] Preparation of human ESC- and iPSC-derived hepatocytes for therapeutic applications and drug toxicity testing in humans should be done in nonxenogenic culture systems to avoid potential contamination with pathogens. Furthermore, the efficiency of the differentiation of the human ESCs and iPSCs into hepatocytes is not particularly high using these methods.[9–14]

In vertebrate development, the liver is derived from the primitive gut tube, which is formed by a flat sheet of cells called the definitive endoderm.[5,15] Shortly afterwards, the definitive endoderm is separated into endoderm derivatives containing the liver bud, the cells of which are referred to as hepatoblasts. The hepatoblasts have the potential to proliferate and differentiate into both hepatocytes and cholangiocytes. In the process of hepatic differentiation, the maturation is characterized by the expression of liver- and stage-specific genes. For example, α-fetoprotein (AFP) is an early hepatic marker, which is expressed in hepatoblasts in the liver bud until birth, and its expression is dramatically reduced after birth.[16] In contrast, albumin (ALB), which is the most abundant protein synthesized by hepatocytes, is initially expressed at lower levels in early fetal hepatocytes, but its expression level is increased as the hepatocytes mature, reaching a maximum in adult hepatocytes.[17] Furthermore, isoforms of cytochrome P450 (CYP) proteins also exhibit differential expression levels according to the developmental stages

Correspondence: *Hiroyuki Mizuguchi, Department of Biochemistry and Molecular Biology, Graduate School of Pharmaceutical Sciences, Osaka University, 1-6 Yamadaoka, Suita, Osaka 565-0871, Japan. E-mail: mizuguch@phs.osaka-u.ac.jp*

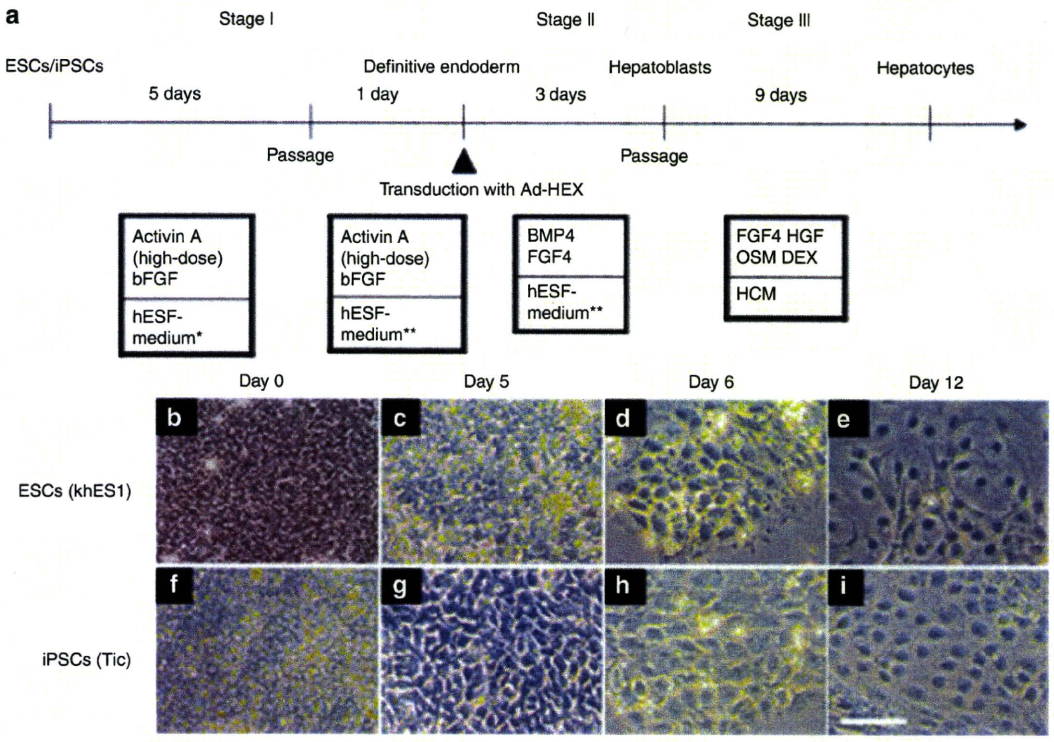

Figure 1 A strategy of differentiation of human embryonic stem cells (ESCs) and induced pluripotent stem cells (iPSCs) to hepatoblasts and hepatocytes. (**a**) Schematic representation illustrating the procedure for differentiation of human ESCs (khES1) and iPSCs (Tic) to hepatocytes. (**b–i**) Phase contrast microscopy showing sequential morphological changes (day 0–12) from (**b–e**) human ESCs (khES1) and (**f–i**) iPSCs (Tic) to hepatoblasts via the definitive endoderm. Bar = 50 µm. bFGF, basic fibroblast growth factor; BMP4, bone morphogenetic protein 4; DEX, dexamethasone; FGF4, fibroblast growth factor 4; HGF, hepatocyte growth factor; OSM, Oncostatin M; HCM, hepatocytes culture medium; *, hESF-GRO medium that was supplemented with 10 µg/ml human recombinant insulin, 5 µg/ml human apotransferrin, 10 µmol/l 2-mercaptoethanol, 10 µmol/l ethanolamine, 10 µmol/l sodium selenite, 0.5 mg/ml fatty acid free BSA; **, hESF-DIF medium that was supplemented with 10 µg/ml insulin, 5 µg/ml apotransferrin, 10 µmol/l 2-mercaptoethanol, 10 µmol/l ethanolamine, 10 µmol/l sodium selenite, 0.5 mg/ml BSA.

of the liver. Although most CYPs (including CYP3A4, CYP7A1, and CYP2D6) are only slightly expressed or not detected in the fetal liver tissue, the expression levels are dramatically increased after birth.[18]

For the development of hepatoblasts, numerous transcription factors are required, such as hematopoietically expressed homeobox (*HEX*), GATA-binding protein 6, prospero homeobox 1, and hepatocyte nuclear factor 4A.[15,19] Among them, *HEX* is suggested to function at the earliest stage of hepatic linage.[20] HEX is first expressed in the definitive endoderm and becomes restricted to the future hepatoblasts. Targeted deletion of the *HEX* gene in the mouse results in embryonic lethality and a dramatic loss of the fetal liver parenchyma.[19,21,22] The hepatic genes, including *ALB*, prospero homeobox1, and hepatocyte nuclear factor 4A, are transiently expressed in the definitive endoderm of *HEX*-null embryos, and further morphogenesis of the hepatoblasts does not occur.[23] In general, then, *HEX* is essential for the definitive endoderm to adopt a hepatic cell fate.

Adenovirus (Ad) vectors are one of the most efficient gene delivery vehicles and have been widely used in both experimental studies and clinical trials.[24] Ad vectors are attractive vehicles for gene transfer because they are easily constructed, can be prepared in high titers, and provide high transduction efficiency in both dividing and nondividing cells. We have developed efficient methods for Ad vector-mediated transient transduction into mouse ESCs and iPSCs.[25,26] We have also showed that the differentiations of mouse ESCs and iPSCs into adipocytes and osteoblasts were dramatically promoted by Ad vector-mediated peroxisome proliferator activated receptor γ and runt related transcription factor 2 transduction, respectively.[25,26]

In this study, we hypothesized that transient *HEX* transduction could efficiently induce hepatoblasts from human ESCs and iPSCs. A previous study demonstrated that *HEX* regulates the differentiation of hemangioblasts and endothelial cells from mouse ESCs,[27] whereas the role of *HEX* in the differentiation of hepatoblasts from human ESCs and iPSCs remains unknown. We found that differentiation of hepatoblasts from the human ESC- and iPSC-derived definitive endoderms, but not from undifferentiated human ESCs and iPSCs, could be facilitated by Ad vector-mediated transient transduction of a *HEX* gene. Furthermore, the Ad-HEX-transduced cells that were derived from human iPSCs were able to differentiate into functional hepatocytes *in vitro*. All the processes for cellular differentiation were performed under serum/feeder cell- free chemically defined conditions. Our culture systems and differentiation method based on Ad vector-mediated transient transduction under chemically defined conditions would provide a platform for drug screening as well as safe therapies.

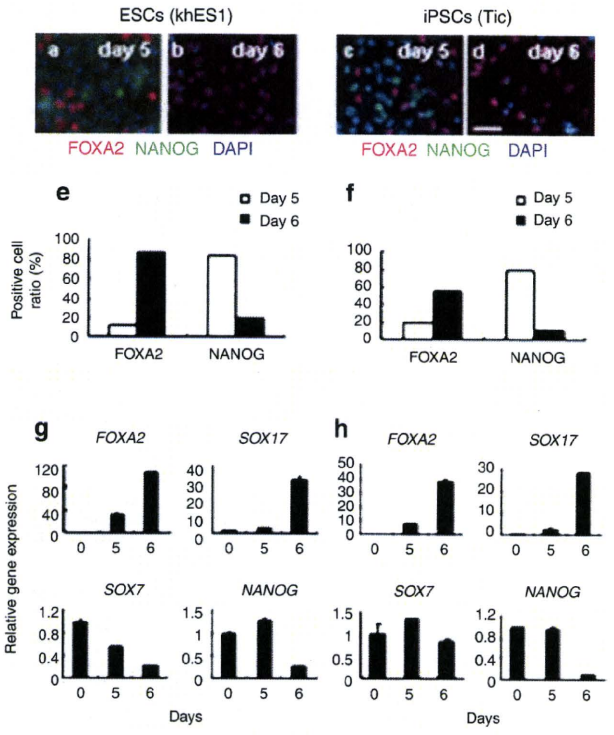

Figure 2 Characterization of the human ESC (khES1)- and iPSC (Tic) derived definitive endoderms. (**a–d**) The immunofluorescent staining of the human ESC (khES1)- and iPSC (Tic) derived differentiated cells before (**a** and **c**; day 5) and after passaging (**b** and **d**; day 6). The cells were immunostained with antibodies against FOXA2 and NANOG. Nuclei were stained with DAPI. (**e,f**) Semiquantitative analysis of the immunofluorescent staining in **a–d**. Data are presented as the mean of immunopositive cells counted in eight independent fields. (**g,h**) Real-time RT-PCR analysis of the level of definitive endoderm (*FOXA2* and *SOX17*), pluripotent (*NANOG*), and extra-embryonic endoderm (*SOX7*) gene expression at day 5 and 6. At day 5, the cells were passaged. Therefore, the data at day 5 and 6 show the levels of gene expression before (at day 5) or after the passage (at day 6). Data are presented as the mean ± SD from triplicate experiments. The graphs represent the relative gene expression level when the level of undifferentiated cells at day 0 was taken as 1. Bar = 50 μm. ESC, embryonic stem cells; iPSC, induced pluripotent stem cells.

RESULTS

Differentiation of human ESC- and iPSC-derived definitive endoderms

Our three-step differentiation protocol is illustrated in **Figure 1a**. After treatment with 50 ng/ml of Activin A (high-dose) and basic fibroblast growth factor (bFGF) for 5 days on a laminin-coated plate, morphologically, the human ESCs and iPSCs were gradually transformed from typical, defined, tight human ESC, and iPSC colonies (day 0) into less dense, flatter cells containing prominent nuclei (day 5), even though the majority of the cells had a morphology resembling that of undifferentiated cells (**Figure 1b,c,f,g**). FACS analysis showed that ~46% of human iPSC-derived differentiated cells expressed CXCR4 (expressed in the definitive endoderm but not the primitive endoderm) (**Supplementary Figure S1a**). Human ESC- and iPSC-derived differentiated cells were immunostained with the definitive endoderm marker, FOXA2 (**Figure 2a,c**). However, the majority of the cells expressed the pluripotent marker NANOG, indicating that undifferentiated cells remain in the induced cultures at day 5. After the cells were passaged with trypsin-EDTA and seeded on a laminin-coated plate a second time, the resultant cells were found to be more homogeneous and flatter at day 6 (**Figure 1d,h**). Semiquantitative analysis by counting immunopositive cells revealed that the number of FOXA2-positive cells was increased and, in turn, the number of NANOG-positive cells was decreased at day 6 after passaging (**Figure 2e,f**). Real-time reverse transcriptase (RT)-PCR analysis showed that the definitive endoderm markers *FOXA2* and *SOX17* mRNA were upregulated, whereas the pluripotent marker *NANOG* mRNA was downregulated at day 6 (**Figure 2g,h**). These results were consistent with the immunofluorescence results (**Figure 2a–d**). The expression levels of the mesoderm marker *FLK1* mRNA and ectoderm marker *PAX6* mRNA were downregulated or unchanged at day 6 (**Supplementary Figure S1b–e**). Importantly, the expression of *SOX7* mRNA (expressed in the extra-embryonic endoderm but not the definitive endoderm) was downregulated (**Figure 2g,h**). These results indicate that the definitive endoderm is induced or selected from human ESCs and iPSCs after passaging. We obtained the same results using another human iPSC line (**Supplementary Figure S2a–d**).

HEX induces hepatoblasts from the human ESC- and iPSC-derived definitive endoderms

To investigate whether forced expression of transcription factors could promote hepatic differentiation, the human ESC- and iPSC-derived definitive endoderms were transduced with Ad vectors. We used a fiber-modified Ad vector containing the elongation factor-1α promoter and a stretch of lysine residue (K7) peptides in the C-terminal region of the fiber knob to examine the transduction efficiency in the human ESC- and iPSC-derived definitive endoderms. The elongation factor-1α promoter was found to be highly active in human ESCs.[28] The K7 peptide targets heparan sulfates on the cellular surface, and the fiber-modified Ad vector containing K7 peptides was shown to be efficient for transduction into many kinds of cells.[29,30] The human ESC- and iPSC-derived definitive endoderms were transduced with a LacZ-expressing Ad vector (Ad-LacZ) at 3,000 vector particle/cell. X-Gal staining showed that the Ad-LacZ-transduced human ESC- and iPSC-derived definitive endoderms successfully expressed LacZ (**Figure 3**). Nearly 100% of the cells transduced with Ad-LacZ were strongly X-gal positive. The transduction efficiency in the human ESC- and iPSC-derived definitive endoderms transduced with the conventional Ad vector containing the wild-type capsid at 3,000 vector particle/cell was ~80% and X-gal staining was much weaker than that in the cells transduced with fiber-modified Ad vectors (**Supplementary Figure S6**).

Next, the human ESC- and iPSC-derived definitive endoderms were transduced with a HEX-expressing fiber-modified Ad vector (Ad-HEX). Although HEX is known to be a transcription factor that is essential for liver development, it remains unclear what the effect of transient *HEX* overexpression is on differentiation from human ESCs and iPSCs or their derivatives *in vitro*. We confirmed the overexpression of *HEX* in the human ESC- and iPSC-derived definitive endoderms transduced with Ad-HEX (**Supplementary Figure S3a–f**). Gene expression analysis revealed the upregulation of *AFP* mRNA, which was expressed by hepatoblasts or early hepatocytes, in Ad-HEX-transduced cells as

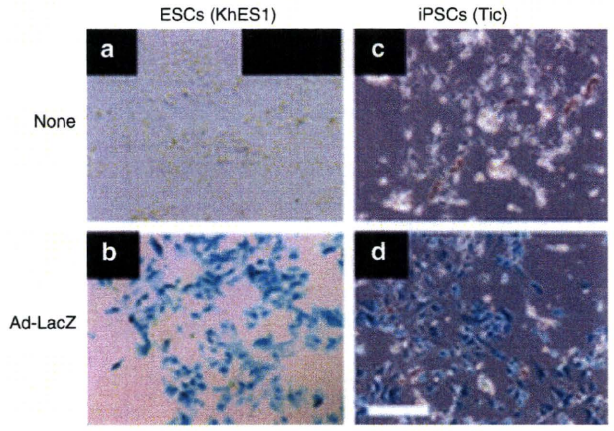

Figure 3 Efficient transgene expression in the human ESC (khES1)- and iPSC (Tic) derived definitive endoderms by using a fiber-modified Ad vector containing the EF-1α promoter. (**a,b**) Human ESC (khES1)-derived and (**c,d**) iPSC (Tic) derived definitive endoderms were transduced with 3,000 VP/cell of Ad-LacZ for 1.5 hours. The next day after transduction, X-gal staining was performed as described in the Materials and Methods section. Similar results were obtained in two independent experiments. Scale = 50 μm. Ad, adenovirus; EF-1α, elongation factor-1α; ESC, embryonic stem cells; iPSC, induced pluripotent stem cells; LacZ, Ad-LacZ-transduced cells; None, nontransduced cells.

compared with nontransduced cells or Ad-LacZ-transduced cells (**Figure 4a,c**). Expression of *ALB* mRNA, which is the most abundant protein in liver, was also observed in Ad-HEX-transduced cells (**Figure 4b,d**).

During liver development, both hepatocytes and cholangiocytes were differentiated from the hepatoblasts. We examined the protein expression of AFP, ALB, and the cholangiocyte marker cytokeratin 7 (CK7) in Ad-HEX-transduced cells by immunostaining (**Figure 4e–p**). The AFP-positive populations were detected in Ad-HEX-transduced cells (**Figure 4g,m**). ALB-positive cells were also detected, although the detection efficiency was very low (**Figure 4j,p**). CK7-positive cells were observed among the Ad-HEX-transduced cells, and all CK7-positive cells were found near the AFP- and ALB-positive cells, suggesting that hepatoblasts are generated by the transient overexpression of a *HEX* gene. Semiquantitative RT-PCR analysis showed that the expression levels of the liver-enriched transcription factors hepatocyte nuclear factor 1A, hepatocyte nuclear factor 1B, hepatocyte nuclear factor 4A, and hepatocyte nuclear factor 6 mRNA were upregulated in Ad-HEX-transduced cells (**Supplementary Figure S4a,b**). The expressions of CCAAT/enhancer binding protein α and prospero homeobox 1 mRNA, two transcription factors known to play a pivotal role in the establishment of the hepatoblasts, were also induced in Ad-HEX-transduced cells (**Supplementary Figure S4a, b**). Taken together, these findings indicate that *HEX* enhances the specification of hepatoblasts from the human ESC- and iPSC-derived definitive endoderms. Similar results were obtained with another human iPSC line (**Supplementary Figure S2e–g**).

Time course of differentiation of the definitive endoderm to hepatoblasts

Next, we examined the time course of AFP and CK7 expression during differentiation of human iPSCs to hepatoblasts in Ad-HEX-

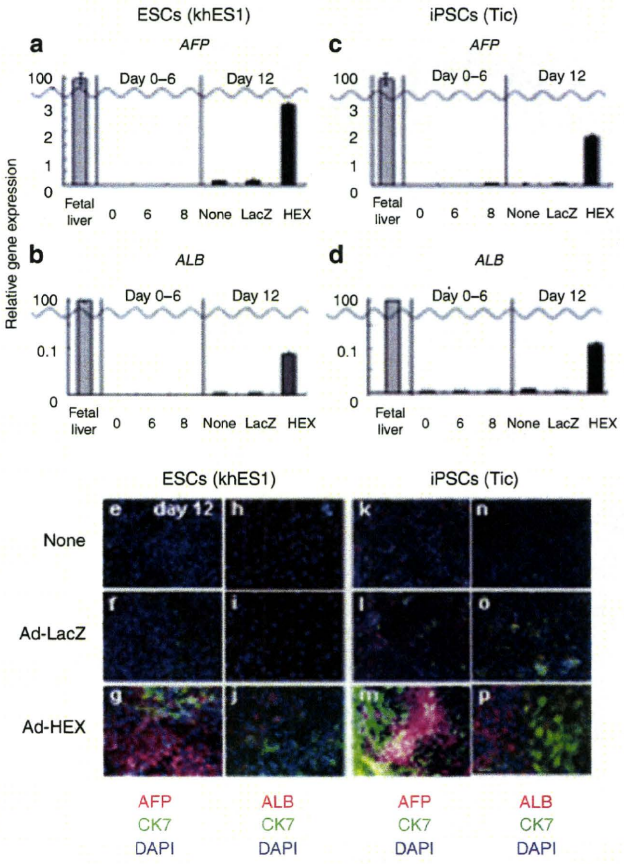

Figure 4 Efficient hepatoblast differentiation from the human ESC (khES1)- and iPSC (Tic) derived definitive endoderms by transduction of the *HEX* gene. (**a–d**) Real-time RT-PCR analysis of the level of (**a,c**) *AFP* and (**b,d**) *ALB* expression in nontransduced cells, Ad-LacZ-transduced cells, and Ad-HEX-transduced cells, all of which were induced from the human ESC (khES1)- and iPSC (Tic) derived definitive endoderms (day 0, 5, 6, and 12). The cells were transduced with Ad-LacZ or Ad-HEX at day 6 as described in **Figure 1a**. The data at day 6 was obtained before the transduction with Ad-HEX. The graphs represent the relative gene expression levels when the level in the fetal liver was taken as 100. (**e–p**) Immunocytochemistry of AFP, ALB, and CK7 expression in nontransduced cells (**e**,**h**,**k**, and **n**), Ad-LacZ-transduced cells (**f**,**i**,**l**, and **o**), and Ad-HEX-transduced cells (**g**,**j**,**m**, and **p**) at day 12, all of which were induced from the human ESC (khES1)- and iPSC (Tic) derived definitive endoderms. Nuclei were stained with DAPI. Bar = 50 μm. Ad, adenovirus; AFP, α-fetoprotein; ALB, albumin; CK7, cytokeratin 7; HEX, Ad-HEX-transduced cells; ESC, embryonic stem cells; iPSC, induced pluripotent stem cell; LacZ, Ad-LacZ-transduced cells; None, nontransduced cells.

transduced cells and nontransduced cells. At day 7 (the day after transduction), the expression of AFP was not detectable in Ad-HEX-transduced or nontransduced cells (**Supplementary Figure S5a,d**). At day 8–9, morphological changes to hepatocyte-like cells were observed in Ad-HEX-transduced cells (**Supplementary Figure S5h,i**). We also observed homogeneous AFP-positive cells at day 9 (**Supplementary Figure S5e**). At day 10, CK7-positive cells appeared, indicating that hepatoblasts started to differentiate into hepatocytes and cholangiocytes at day 9–10 (**Supplementary Figure S5f**). At day 12, ALB-positive cells appeared, indicating that hepatocytes were differentiated from Ad-HEX-transduced cells (**Figure 4p**). These results showed that *HEX* induces the hepatoblasts from the

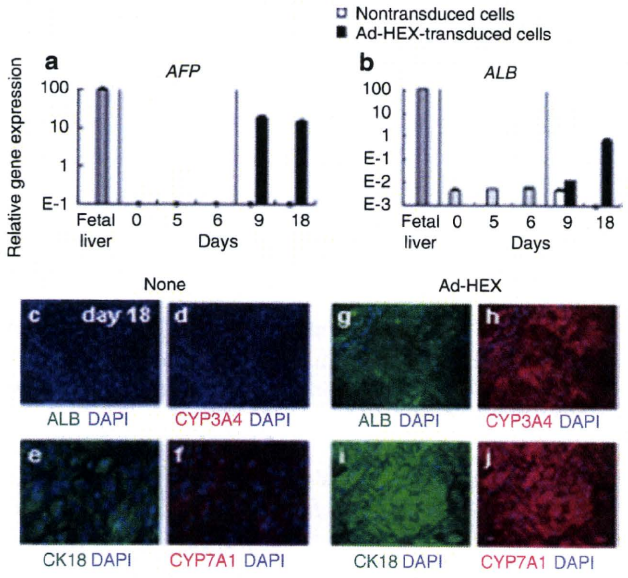

Figure 5 Efficient differentiation of Ad-HEX-transduced hepatoblasts into hepatocytes. (**a**,**b**) Real-time RT-PCR analysis of (**a**) *AFP* and (**b**) *ALB* expression in nontransduced cells and Ad-HEX-transduced cells, both of which were induced from the human iPSC (Tic) derived definitive endoderm (day 0, 5, 6, and 12). The cells were transduced with Ad-HEX at day 6 as described in **Figure 1a**. The data at day 6 were obtained before the transduction with Ad-HEX. The graphs represent the relative gene expression level when the level in the fetal liver was taken as 100. (**c–j**) Immunocytochemistry of ALB, CYP3A4, CYP7A1, and CK18 expression in (**c–f**) nontransduced cells and (**g–j**) Ad-HEX-transduced cells, all of which were induced from the human iPSC (Tic) derived definitive endoderm at day 18. Nuclei were stained with DAPI. Bar = 50μm. Ad, adenovirus; AFP, α-fetoprotein; ALB, albumin; CK18, cytokeratin 18; ESC, embryonic stem cells; HEX, Ad-HEX-transduced cells; iPSC, induced pluripotent stem cell; None, nontransduced cells; RT-PCR, reverse transcriptase-PCR.

definitive endoderm, and the Ad-HEX-transduced cells could differentiate into both hepatocytes and cholangiocytes.

Directed hepatic differentiation from hepatoblasts

With the protocol described above, heterogeneous populations containing CK7-positive cholangiocytes were observed at day 12 (**Figure 4p**). To promote the differentiation of hepatoblasts to hepatocytes, the human iPSC-derived differentiated cells at day 9 (**Supplementary Figure S5e**) were dislodged with trypsin-EDTA and plated on collagen I-coated dishes as previously reported.[11] After 8–11 days in culture with medium containing FGF4, HGF, OSM, and DEX, the Ad-HEX-transduced cells became more flattened (**Supplementary Figure S5m**), whereas the nontransduced cells became fibroblast-like cells (**Supplementary Figure S5i**). Gene expression analysis showed the upregulation of *ALB* mRNA in Ad-HEX-transduced cells under this culture condition, whereas the expression of *ALB* mRNA was reduced in the nontransduced cells at day 18 (**Figure 5b**). Immunostaining showed that only a small percentage of Ad-HEX-transduced cells expressed ALB at day 12 (**Figure 4p**), whereas most of the Ad-HEX-transduced cells were ALB-positive at day 18 (**Figure 5g**). Most of the Ad-HEX-transduced cells also expressed CYP3A4 at day 18 (**Figure 5h**). More importantly, in the Ad-HEX-transduced cells, CYP7A1 and cytokeratin 18 were detected and these proteins are known

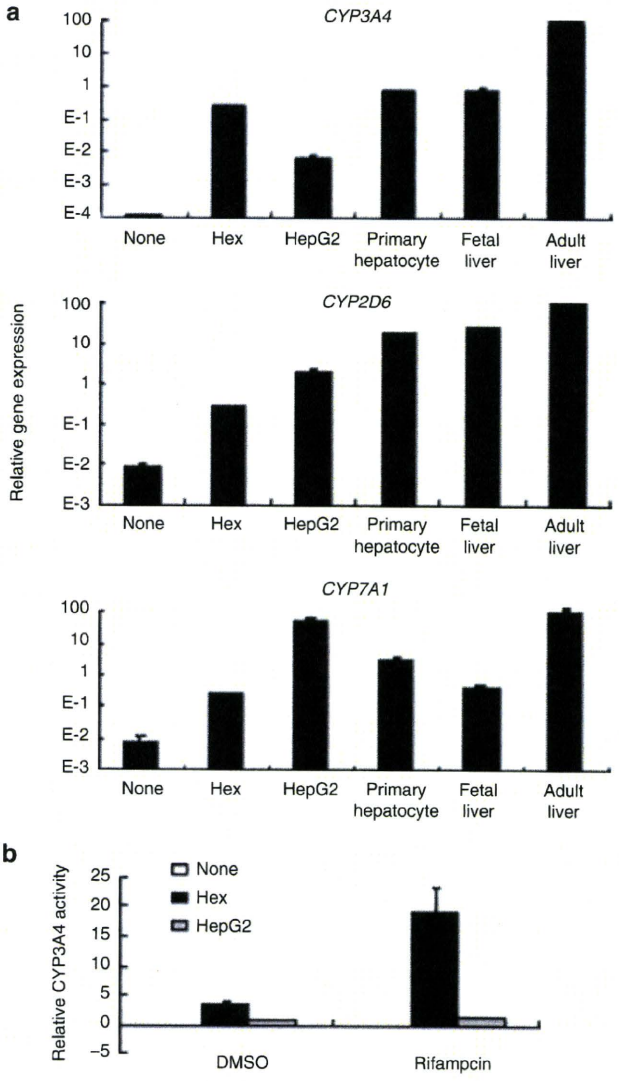

Figure 6 Cytochrome P450 isozymes in human iPSC (Tic) derived hepatocytes. (**a**) Real-time RT-PCR analysis of *CYP3A4*, *CYP7A1*, and *CYP2D6* expression in iPSC (Tic) derived nontransduced cells, Ad-HEX-transduced cells, and fetal and adult liver tissues. (**b**) Induction of CYP3A4 by rifampicin in human iPSC (Tic) derived nontransduced cells, Ad-HEX-transduced cells, the HepG2 cell line and primary human hepatocytes, which were cultured 48 hours after plating the cells. Data are presented as the mean ± SD from triplicate experiments. The graphs represent the relative gene expression level when the level in the adult liver was taken as 100. AFP, α-fetoprotein; ALB, albumin; DMSO, dimethyl sulfoxide; ESC, embryonic stem cells; HEX, Ad-HEX-transduced cells; iPSC, induced pluripotent stem cell; LacZ, Ad-LacZ-transduced cells; None, nontransduced cells.

to be detected in hepatocytes but not in extra-embryonic cells[31,32] (**Figure 5i,j**). Quantitative analysis showed that ~84, 80, 88, and 92% of Ad-HEX-transduced cells expressed ALB, CYP3A4, CYP7A1, and cytokeratin 18, respectively. These results indicate that Ad-HEX-transduced cells could differentiate to hepatic cells. However, the expression level of *ALB* mRNA in Ad-HEX-transduced cells was lower than that in fetal liver tissue and in turn, the expression of *AFP* mRNA was maintained (**Figure 5a**). Therefore, Ad-HEX-transduced cells are committed to the hepatic linage, but are not yet mature hepatocytes.

Ad-HEX-transduced cells exhibit hepatic functions

To test the hepatic function in the Ad-HEX-transduced cells, we investigated the liver metabolism, because P450 cytochrome enzymes play a critical role in this function. We examined the expression level of several members of this multigene family, *i.e.*, *CYP3A4*, *CYP7A1*, mRNA and *CYP2D6* in Ad-HEX-transduced cells by real-time RT-PCR. The real-time RT-PCR analysis showed that the mRNAs for *CYP3A4*, *CYP7A1*, and *CYP2D6* were expressed in Ad-HEX-transduced cells, whereas none of these mRNAs were expressed in the nontransduced cells (**Figure 6a**). The expression levels of *CYP3A4* in Ad-HEX-transduced cells were similar to those observed in primary human hepatocytes, which were cultured 48 hours after plating the cells, or fetal liver tissues but lower than those in adult liver. The *CYP2D6* and *CYP7A1* mRNA expressions in Ad-HEX-transduced cells were lower than those in primary hepatocytes or adult tissues. Next, we investigated the metabolism of the P450 3A4 substrates by measuring the activity of P450 isozymes. The metabolites were detected in Ad-HEX-transduced cells, and their activity was 3.4-fold higher than that in the most commonly used human hepatocyte cell line, HepG2 (**Figure 6b**; DMSO column). This result was consistent with the real-time RT-PCR data (**Figure 6a**). We further tested the induction of CYP3A4 upon chemical stimulation, because CYP3A4 is the most prevalent P450 isozyme in the liver and is involved in the metabolism of a significant proportion of the currently available commercial drugs. Because CYP3A4 can be induced with rifampicin, both Ad-HEX-transduced cells and HepG2 cells were treated with rifampicin, followed by treatment with CYP3A4 substrate. Ad-HEX-transduced cells produced 5.4-fold higher levels of metabolites in response to rifampicin treatment (**Figure 6b**; rifampicin column). This result indicates that P450 isozymes are active in Ad-HEX-transduced cells.

DISCUSSION

The object of this study was to develop an efficient method for generating hepatoblasts and hepatocytes from human ESCs and iPSCs for application to drug toxicity screening tests as well as therapeutics such as regenerative medicine. We found that transient HEX transduction in the definitive endoderm together with a culture under chemically defined conditions was useful for this purpose.

It has been reported that a high concentration of Activin A induces differentiation of human ESCs into the definitive endoderm.[8,33,34] On the other hand, undifferentiated human ESCs are maintained by a low concentration of Activin A.[35] Several studies have shown that bFGF promotes the differentiation of ESCs into the definitive endoderm and inhibits the differentiation of ESCs into the extra-embryonic endoderm.[35–38] bFGF has been reported to inhibit the BMP signaling, which can promote the extra-embryonic lineage differentiation.[39] The extra-embryonic endoderm expresses most of the hepatocyte markers, such as AFP.[40] Contamination of the extra-embryonic endoderm makes it difficult to estimate the hepatic differentiation from human ESCs and iPSCs.[11,14,40] In this study, we showed that both Activin A and bFGF induce definitive endoderm populations, while they repress the extra-embryonic endoderm differentiation (**Figure 2g,h**). Interestingly, after the differentiated cells that were cultured on laminin-coated plates with Activin A and bFGF were passaged at day 5, FOXA2-positive cells (definitive endoderm) were enriched in the resultant cells at day 6 (**Figure 2a–f**). This may have been because FOXA2-positive cells efficiently adhered to the laminin-coated plate and/or because trypsinized, single undifferentiated ESCs/iPSCs cannot survive. The passaging of differentiated cells might be attributed to the reduction in the number of not only the extra-embryonic endoderm cells but also the undifferentiated cells. However, the efficiency of the definitive endoderm differentiation in this study was not as efficient as that reported by other groups.[8,33,34] Other cell lineages, such as the mesoderm and extra-embryonic endoderm, might remain at day 6 (**Figure 2g,h** and **Supplementary Figure S1**). Further improvement of the culture conditions will thus be needed in order to enhance the definitive endoderm differentiation.

Hepatoblasts and hepatocytes were differentiated from the human ESC- and iPSC-derived definitive endoderms by transient overexpression of the homeobox gene *HEX*. A fiber-modified Ad vector containing K7 peptides mediated much higher gene expression than conventional Ad vectors in the human ESC- and iPSC-derived definitive endoderms (**Supplementary Figure S6**). This new hepatic differentiation protocol shows that *HEX* induces AFP-positive hepatoblasts at day 9 and ALB-positive hepatocytes at day 12 from human ESCs and iPSCs, whereas the previous protocols require a few weeks or months to induce AFP- and ALB-positive hepatocytes from PSCs.[9–11] Previous studies suggested that *HEX* could regulate liver-enriched transcription factors such as hepatocyte nuclear factor 4A and hepatocyte nuclear factor 6.[19,23] Overexpression of the *HEX* gene under the conditions employed in the present study could activate several transcription factors that are required for hepatic differentiation (**Supplementary Figure S4a,b**). However, the Ad-HEX-transduced cells showed a low level of expression of *ALB* and some CYP450 species, as well as a high level of *AFP* expression, indicating that the cells were still immature. To promote further hepatic differentiation or maturation, it may be effective to culture the hepatic cells in a 3D environment or on feeder cells such as cardiomyocyte- or endothelium-derived cells.[41,42] In addition, the function of our hepatic cells was still limited. Further analysis of the other functions of our hepatic cells, such as glycogen storage, uptake of indocyanine green and organic anion low-density lipoprotein, and transplantation of Ad-HEX-transduced cells into the liver of immunodeficient mice, is clearly needed for the appreciation to drug screening and therapeutic treatment modalities.

During the preparation of this article, Kubo *et al.* have reported that *HEX* could promote hepatoblast differentiation from mouse ESCs.[43] Their report is consistent with our data, suggesting that *HEX* plays a pivotal regulatory role in not only mouse but also human hepatic differentiation. They also showed that the overexpression of *HEX* at the definitive endoderm stage is critical for hepatic specification of the mouse ESCs. We also confirmed that forced expression of *HEX* in the undifferentiated human ESCs and iPSCs did not elevate the expression of *ALB* and *CK7* (**Supplementary Figure S7**), indicating that *HEX* enhances the hepatic differentiation not from the undifferentiated cells but from the definitive endoderm. However, Kubo *et al.* used recombinant mouse ESCs (tet-HEX ESCs), in which the tetracycline-regulated *HEX* expression cassette

is integrated into the host cell genome to induce *HEX* in a stage-specific manner. Their system would not be appropriate for clinical use because the transgene is randomly integrated into the host cell genome and this leads to a risk of mutagenesis.[44] On the other hand, we generated human hepatoblasts by Ad vector-mediated transient *HEX* transduction, method which avoids the integration of exogenous DNA into the host chromosome.

Touboul *et al.* reported that human ESCs and iPSCs can differentiate into functional hepatocytes under chemically defined conditions.[34] In the present study, hepatoblasts were generated in a chemically defined serum-free medium, which minimized exposure to animal cells and proteins, and on a defined extracellular matrix, such as laminin or collagen, which do not contain undefined growth factors. To generate hepatocytes, hepatocyte culture medium, which is serum-free but not defined, was used in the stage III. When defined hESF-medium was used in the stage III, the expression levels of *ALB* and *CYP3A4* mRNA were half the levels seen in the cells cultured with hepatocyte culture medium in the preliminary experiment (data not shown). Human ESCs and iPSCs were also grown for maintaining the undifferentiated state on a feeder layer, which contains xenoantigen such as bovine apolipoprotein B-100. Bovine apolipoprotein B-100 is known to be a dominant xenoantigen for cell-based therapies.[45] Human ESC- and iPSC-derived hepatocytes should be generated and cultured under chemically defined conditions not only to avoid potential contamination with pathogens for the safer therapeutic application, but also to obtain reproducible results using the differentiation protocols.[34,46] Development of differentiation protocols using other genes of transcription factors as well as *HEX* genes based on a chemically defined medium is under way. Overall, our strategy should provide a novel protocol for hepatic differentiation from human ESCs and iPSCs, which could be useful for regenerative medicine and drug screening.

MATERIALS AND METHODS

Ad vectors. Ad vectors were constructed by an improved *in vitro* ligation method.[47,48] The human *HEX* complementary DNA derived from pDNR-LIB-*HEX* (Invitrogen, Carlsbad, CA) was inserted into pHMEF5,[29] which contains the human elongation factor-1α promoter, resulting in pHMEF-HEX. The pHMEF-HEX was digested with I-CeuI/PI-SceI and ligated into I-CeuI/PI-SceI-digested pAdHM41-K7,[30] resulting in pAd-HEX. Ad-HEX and Ad-LacZ, both of which contain the elongation factor-1α promoter and a stretch of lysine residues (K7) peptides in the C-terminal region of the fiber knob, were generated and purified as described previously.[26,29] The vector particle titer was determined by using a spectrophotometric method.[49]

Human ESCs and iPSCs culture. A human ESC line, khES1, was obtained from Kyoto University (Kyoto, Japan).[50] khES1 was used following the Guidelines for Derivation and Utilization of Human Embryonic Stem Cells of the Ministry of Education, Culture, Sports, Science and Technology of Japan after approval by the review board at Kyoto University. Human ESCs were maintained on a feeder layer of mitomycin-inactivated mouse embryonic fibroblasts (ICR; ReproCELL Incorporated, Tokyo, Japan) with Dulbecco's modified Eagle's medium/F-12 (Sigma, St Louis, MO) supplemented with 0.1 mmol/l 2-mercaptoethanol, 0.1 mmol/l nonessential amino acids, 2 mmol/l L-glutamine, 20% GIBCO knockout serum replacement (Invitrogen), and 5 ng/ml bFGF (Sigma) in a humidified atmosphere of 3% CO_2 and 97% air at 37 °C. Human ESCs were dissociated with 0.1 mg/ml dispase (Roche Diagnostics, Burgess Hill, UK) into small clumps, and subcultured every 5 or 6 days.

Two human iPS clones derived from the embryonic human lung fibroblast cell line MCR5 were provided from JCRB Cell Bank (Tic, JCRB Number: JCRB1331; and Dotcom, JCRB Number: JCRB1327).[3,4] In the present study, we mainly used the Tic cell line, but similar results were obtained using the Dotcom cell line, and these are shown in the supplementary figures. Human iPSCs were maintained on a feeder layer of mitomycin-inactivated mouse embryonic fibroblasts (Hygro Resistant Strain C57/BL6; Hygro, Millipore, MA) on a gelatin-coated flask in human iPS medium. Human iPS medium consists of knockout Dulbecco's modified Eagle's medium/F12 (Invitrogen), supplemented with 0.1 mmol/l 2-mercaptoethanol, 0.1 mmol/l nonessential amino acids, 2 mmol/l L-glutamine, 20% knockout serum replacement, and 10 ng/ml bFGF in a humidified atmosphere of 5% CO_2 and 95% air at 37 °C. Human iPSCs were dissociated with 0.1 mg/ml dispase (Roche) into small clumps and subcultured every 7 or 8 days.

In vitro *differentiation.* Before the initiation of cellular differentiation, the medium of human ESCs and iPSCs was exchanged for a defined serum-free medium hESF9 and cultured in a humidified atmosphere of 10% CO_2 and 90% air at 37 °C.[46] hESF9 consists of hESF-GRO medium (Cell Science & Technology Institute, Sendai, Japan) supplemented with five factors (10 μg/ml human recombinant insulin, 5 μg/ml human apotransferrin, 10 μmol/l 2-mercaptoethanol, 10 μmol/l ethanolamine, 10 μmol/l sodium selenite), oleic acid conjugated with fatty acid free bovine ALB, 10 ng/ml bFGF, and 100 ng/ml heparin (all from Sigma). For induction of definitive endoderm, human ESCs and iPSCs were dissociated into single cells with Accutase (Invitrogen) and cultured for 5 days on a mouse laminin-coated tissue 12-well plate (6.0×10^4 cells/cm^2) in hESF-GRO medium (Cell Science & Technology Institute) supplemented with the five factors, 0.5 mg/ml fatty acid free bovine ALB (BSA) (Sigma), 10 ng/ml bFGF, and 50 ng/ml Activin A (R&D Systems, Minneapolis, MN) in a humidified atmosphere of 10% CO_2 and 90% air at 37 °C. The medium was refreshed every day.

For induction of hepatoblasts, the human ESC- and iPSC-derived definitive endoderms (day 5) were dissociated with 0.0125% trypsin-0.01325 mmol/l EDTA, and then the trypsin was inactivated with 0.1% soybean trypsin inhibitor (Sigma). The cells were seeded at 1.2×10^5 cells/cm^2 on a laminin-coated 12-well plate with hESF-DIF (Cell Science & Technology Institute) medium supplemented with the five factors, 0.5 mg/ml BSA, 10 ng/ml bFGF, and 50 ng/ml Activin A in a humidified atmosphere of 10% CO_2 and 90% air at 37 °C. The next day, the cells were transduced with 3,000 vector particle/cell of Ad vectors (Ad-HEX and Ad-LacZ) for 1.5 hours in hESF-DIF medium supplemented with the five factors, BSA, 10 ng/ml FGF4 (R&D Systems) and 10 ng/ml BMP4 (R&D Systems).[10] The medium was refreshed every day.

For induction of hepatocytes, human iPSC-derived hepatoblasts in one well (day 9) were passaged onto two wells with 0.0125% trypsin-0.01325mmol/l EDTA and 0.1% trypsin inhibitor, on type I collagen-coated tissue 12-well plate (15 μg/cm^2) (Nitta Gelatin, Osaka, Japan). The cells were cultured in hepatocyte culture medium supplemented with SingleQuots (Lonza, Walkersville, MD), 10 ng/ml FGF4, 10 ng/ml HGF (R&D Systems), 10 ng/ml Oncostatin M (R&D Systems), and 0.392 ng/ml dexamethasone (Sigma).[11] The medium was refreshed every 2 days.

RNA isolation, RT-PCR, immunostaining, flow cytometry, lacz assay, and assay for cytochrome P4503A4 activity. For details of these procedures, See **Supplementary Materials and Methods, Supplementary Tables S1 and S2.**

SUPPLEMENTARY MATERIAL

Figure S1. Characterization of the human ESC (khES1)- and iPSC (Tic)-derived definitive endoderms.

Figure S2. Efficient differentiation of another human iPSC line (Dotcom) into hepatoblasts by overexpression of the *HEX* gene.

Figure S3. Overexpression of *HEX* in the human ESC (khES1)- and iPSC (Tic)-derived definitive endoderms.

Figure S4. Characterization of Ad-HEX-transduced hepatoblasts.
Figure S5. Progression of differentiation of the definitive endoderm to hepatoblasts.
Figure S6. X-gal staining of human iPSC (Tic)-derived definitive endoderms transduced with a conventional or a fiber-modified Ad vector containing the EF-1α promoter.
Figure S7. *HEX* promotes the differentiation into the hepatic lineage, not from undifferentiated iPSCs (Tic), but from iPSC (Tic)-derived definitive endoderm.
Table S1. List of Taqman gene expression assays and primers.
Table S2. List of antibodies used.
Materials and Methods.

ACKNOWLEDGMENTS

We thank Hiroko Matsumura and Midori Hayashida for their excellent technical support. This study was supported by grants from the Ministry of Education, Sports, Science and Technology of Japan (20200076) and by grants from the Ministry of Health, Labor, and Welfare of Japan.

REFERENCES

1. Thomson, JA, Itskovitz-Eldor, J, Shapiro, SS, Waknitz, MA, Swiergiel, JJ, Marshall, VS *et al.* (1998). Embryonic stem cell lines derived from human blastocysts. *Science* **282**: 1145–1147.
2. Takahashi, K, Tanabe, K, Ohnuki, M, Narita, M, Ichisaka, T, Tomoda, K *et al.* (2007). Induction of pluripotent stem cells from adult human fibroblasts by defined factors. *Cell* **131**: 861–872.
3. Makino, H, Toyoda, M, Matsumoto, K, Saito, H, Nishino, K, Fukawatase, Y *et al.* (2009). Mesenchymal to embryonic incomplete transition of human cells by chimeric OCT4/3 (POU5F1) with physiological co-activator EWS. *Exp Cell Res* **315**: 2727–2740.
4. Nagata, TM, Yamaguchi, S, Hirano, K, Makino, H, Nishino, K, Miyagawa, Y *et al.* (2009). Efficient reprogramming of human and mouse primary extra-embryonic cells to pluripotent stem cells. *Genes Cells* **14**: 1395–1404.
5. Lavon, N and Benvenisty, N (2005). Study of hepatocyte differentiation using embryonic stem cells. *J Cell Biochem* **96**: 1193–1202.
6. Khetani, SR and Bhatia, SN (2008). Microscale culture of human liver cells for drug development. *Nat Biotechnol* **26**: 120–126.
7. Baharvand, H, Hashemi, SM and Shahsavani, M (2008). Differentiation of human embryonic stem cells into functional hepatocyte-like cells in a serum-free adherent culture condition. *Differentiation* **76**: 465–477.
8. Hay, DC, Zhao, D, Fletcher, J, Hewitt, ZA, McLean, D, Urruticoechea-Uriguen, A *et al.* (2008). Efficient differentiation of hepatocytes from human embryonic stem cells exhibiting markers recapitulating liver development in vivo. *Stem Cells* **26**: 894–902.
9. Shiraki, N, Umeda, K, Sakashita, N, Takeya, M, Kume, K and Kume, S (2008). Differentiation of mouse and human embryonic stem cells into hepatic lineages. *Genes Cells* **13**: 731–746.
10. Song, Z, Cai, J, Liu, Y, Zhao, D, Yong, J, Duo, S *et al.* (2009). Efficient generation of hepatocyte-like cells from human induced pluripotent stem cells. *Cell Res* **19**: 1233–1242.
11. Agarwal, S, Holton, KL and Lanza, R (2008). Efficient differentiation of functional hepatocytes from human embryonic stem cells. *Stem Cells* **26**: 1117–1127.
12. Si-Tayeb, K, Noto, FK, Nagaoka, M, Li, J, Battle, MA, Duris, C *et al.* (2010). Highly efficient generation of human hepatocyte-like cells from induced pluripotent stem cells. *Hepatology* **51**: 297–305.
13. Duan, Y, Ma, X, Zou, W, Wang, C, Bahbahan, IS, Ahuja, TP *et al.* (2010). Differentiation and characterization of metabolically functioning hepatocytes from human embryonic stem cells. *Stem Cells* **28**: 674–686.
14. Cai, J, Zhao, Y, Liu, Y, Ye, F, Song, Z, Qin, H *et al.* (2007). Directed differentiation of human embryonic stem cells into functional hepatic cells. *Hepatology* **45**: 1229–1239.
15. McLin, VA and Zorn, AM (2006). Molecular control of liver development. *Clin Liver Dis* **10**: 1–25, v.
16. Shiojiri, N (1981). Enzymo- and immunocytochemical analyses of the differentiation of liver cells in the prenatal mouse. *J Embryol Exp Morphol* **62**: 139–152.
17. Shiojiri, N (1984). The origin of intrahepatic bile duct cells in the mouse. *J Embryol Exp Morphol* **79**: 25–39.
18. Ingelman-Sundberg, M, Oscarson, M and McLellan, RA (1999). Polymorphic human cytochrome P450 enzymes: an opportunity for individualized drug treatment. *Trends Pharmacol Sci* **20**: 342–349.
19. Hunter, MP, Wilson, CM, Jiang, X, Cong, R, Vasavada, H, Kaestner, KH *et al.* (2007). The homeobox gene Hhex is essential for proper hepatoblast differentiation and bile duct morphogenesis. *Dev Biol* **308**: 355–367.
20. Bogue, CW, Ganea, GR, Sturm, E, Ianucci, R and Jacobs, HC (2000). Hex expression suggests a role in the development and function of organs derived from foregut endoderm. *Dev Dyn* **219**: 84–89.
21. Martinez Barbera, JP, Clements, M, Thomas, P, Rodriguez, T, Meloy, D, Kioussis, D *et al.* (2000). The homeobox gene Hex is required in definitive endodermal tissues for normal forebrain, liver and thyroid formation. *Development* **127**: 2433–2445.
22. Keng, VW, Yagi, H, Ikawa, M, Nagano, T, Myint, Z, Yamada, K *et al.* (2000). Homeobox gene Hex is essential for onset of mouse embryonic liver development and differentiation of the monocyte lineage. *Biochem Biophys Res Commun* **276**: 1155–1161.
23. Bort, R, Signore, M, Tremblay, K, Martinez Barbera, JP and Zaret, KS (2006). Hex homeobox gene controls the transition of the endoderm to a pseudostratified, cell emergent epithelium for liver bud development. *Dev Biol* **290**: 44–56.
24. Xu, ZL, Mizuguchi, H, Sakurai, F, Koizumi, N, Hosono, T, Kawabata, K *et al.* (2005). Approaches to improving the kinetics of adenovirus-delivered genes and gene products. *Adv Drug Deliv Rev* **57**: 781–802.
25. Tashiro, K, Inamura, M, Kawabata, K, Sakurai, F, Yamanishi, K, Hayakawa, T *et al.* (2009). Efficient adipocyte and osteoblast differentiation from mouse induced pluripotent stem cells by adenoviral transduction. *Stem Cells* **27**: 1802–1811.
26. Tashiro, K, Kawabata, K, Sakurai, H, Kurachi, S, Sakurai, F, Yamanishi, K *et al.* (2008). Efficient adenovirus vector-mediated PPAR gene transfer into mouse embryoid bodies promotes adipocyte differentiation. *J Gene Med* **10**: 498–507.
27. Kubo, A, Chen, V, Kennedy, M, Zahradka, E, Daley, GQ and Keller, G (2005). The homeobox gene HEX regulates proliferation and differentiation of hemangioblasts and endothelial cells during ES cell differentiation. *Blood* **105**: 4590–4597.
28. Kovesdi, I, Brough, DE, Bruder, JT and Wickham, TJ (1997). Adenoviral vectors for gene transfer. *Curr Opin Biotechnol* **8**: 583–589.
29. Kawabata, K, Sakurai, F, Yamaguchi, T, Hayakawa, T and Mizuguchi, H (2005). Efficient gene transfer into mouse embryonic stem cells with adenovirus vectors. *Mol Ther* **12**: 547–554.
30. Koizumi, N, Mizuguchi, H, Utoguchi, N, Watanabe, Y and Hayakawa, T (2003). Generation of fiber-modified adenovirus vectors containing heterologous peptides in both the HI loop and C terminus of the fiber knob. *J Gene Med* **5**: 267–276.
31. Asahina, K, Fujimori, H, Shimizu-Saito, K, Kumashiro, Y, Okamura, K, Tanaka, Y *et al.* (2004). Expression of the liver-specific gene Cyp7a1 reveals hepatic differentiation in embryoid bodies derived from mouse embryonic stem cells. *Genes Cells* **9**: 1297–1308.
32. Moll, R, Franke, WW, Schiller, DL, Geiger, B and Krepler, R (1982). The catalog of human cytokeratins: patterns of expression in normal epithelia, tumors and cultured cells. *Cell* **31**: 11–24.
33. D'Amour, KA, Agulnick, AD, Eliazer, S, Kelly, OG, Kroon, E and Baetge, EE (2005). Efficient differentiation of human embryonic stem cells to definitive endoderm. *Nat Biotechnol* **23**: 1534–1541.
34. Touboul, T, Hannan, NR, Corbineau, S, Martinez, A, Martinet, C, Branchereau, S *et al.* (2010). Generation of functional hepatocytes from human embryonic stem cells under chemically defined conditions that recapitulate liver development. *Hepatology* **51**: 1754–1765.
35. Vallier, L, Touboul, T, Brown, S, Cho, C, Bilican, B, Alexander, M *et al.* (2009). Signaling pathways controlling pluripotency and early cell fate decisions of human induced pluripotent stem cells. *Stem Cells* **27**: 2655–2666.
36. Shiraki, N, Yoshida, T, Araki, K, Umezawa, A, Higuchi, Y, Goto, H *et al.* (2008). Guided differentiation of embryonic stem cells into Pdx1-expressing regional-specific definitive endoderm. *Stem Cells* **26**: 874–885.
37. Morrison, GM, Oikonomopoulou, I, Migueles, RP, Soneji, S, Livigni, A, Enver, T *et al.* (2008). Anterior definitive endoderm from ESCs reveals a role for FGF signaling. *Cell Stem Cell* **3**: 402–415.
38. Sumi, T, Tsuneyoshi, N, Nakatsuji, N and Suemori, H (2008). Defining early lineage specification of human embryonic stem cells by the orchestrated balance of canonical Wnt/beta-catenin, Activin/Nodal and BMP signaling. *Development* **135**: 2969–2979.
39. Xu, RH, Peck, RM, Li, DS, Feng, X, Ludwig, T and Thomson, JA (2005). Basic FGF and suppression of BMP signaling sustain undifferentiated proliferation of human ES cells. *Nat Methods* **2**: 185–190.
40. Keller, G (2005). Embryonic stem cell differentiation: emergence of a new era in biology and medicine. *Genes Dev* **19**: 1129–1155.
41. Selden, C, Shariat, A, McCloskey, P, Ryder, T, Roberts, E and Hodgson, H (1999). Three-dimensional *in vitro* cell culture leads to a marked upregulation of cell function in human hepatocyte cell lines–an important tool for the development of a bioartificial liver machine. *Ann N Y Acad Sci* **875**: 353–363.
42. Soto-Gutiérrez, A, Navarro-Alvarez, N, Zhao, D, Rivas-Carrillo, JD, Lebkowski, J, Tanaka, N *et al.* (2007). Differentiation of mouse embryonic stem cells to hepatocyte-like cells by co-culture with human liver nonparenchymal cell lines. *Nat Protoc* **2**: 347–356.
43. Kubo, A, Kim, YH, Irion, S, Kasuda, S, Takeuchi, M, Ohashi, K *et al.* (2010). The homeobox gene Hex regulates hepatocyte differentiation from embryonic stem cell-derived endoderm. *Hepatology* **51**: 633–641.
44. Hacein-Bey-Abina, S, Von Kalle, C, Schmidt, M, McCormack, MP, Wulffraat, N, Leboulch, P *et al.* (2003). LMO2-associated clonal T cell proliferation in two patients after gene therapy for SCID-X1. *Science* **302**: 415–419.
45. Sakamoto, N, Tsuji, K, Muul, LM, Lawler, AM, Petricoin, EF, Candotti, F *et al.* (2007). Bovine apolipoprotein B-100 is a dominant immunogen in therapeutic cell populations cultured in fetal calf serum in mice and humans. *Blood* **110**: 501–508.
46. Furue, MK, Na, J, Jackson, JP, Okamoto, T, Jones, M, Baker, D *et al.* (2008). Heparin promotes the growth of human embryonic stem cells in a defined serum-free medium. *Proc Natl Acad Sci USA* **105**: 13409–13414.
47. Mizuguchi, H and Kay, MA (1998). Efficient construction of a recombinant adenovirus vector by an improved *in vitro* ligation method. *Hum Gene Ther* **9**: 2577–2583.
48. Mizuguchi, H and Kay, MA (1999). A simple method for constructing E1- and E1/E4-deleted recombinant adenoviral vectors. *Hum Gene Ther* **10**: 2013–2017.
49. Maizel, JV Jr, White, DO and Scharff, MD (1968). The polypeptides of adenovirus. I. Evidence for multiple protein components in the virion and a comparison of types 2, 7A, and 12. *Virology* **36**: 115–125.
50. Suemori, H, Yasuchika, K, Hasegawa, K, Fujioka, T, Tsuneyoshi, N and Nakatsuji, N (2006). Efficient establishment of human embryonic stem cell lines and long-term maintenance with stable karyotype by enzymatic bulk passage. *Biochem Biophys Res Commun* **345**: 926–932.

—Review—

iPS細胞への遺伝子導入を用いた分化誘導の最適化

川端健二,*,[a,b] 田代克久,[a] 水口裕之[a,c]

Differentiation of Functional Cells from iPS Cells by Efficient Gene Transfer

Kenji KAWABATA,*,[a,b] Katsuhisa TASHIRO,[a] and Hiroyuki MIZUGUCHI[a,c]

[a]*Laboratory of Stem Cell Regulation, National Institute of Biomedical Innovation, 7-6-8 Saito-Asagi, Ibaraki, Osaka 567-0085, Japan,* [b]*Department of Biomedical Innovation and* [c]*Department of Biochemistry and Molecular Biology, Graduate School of Pharmaceutical Sciences, Osaka University, 1-6 Yamadaoka, Suita, Osaka 565-0871, Japan*

(Received July 20, 2010)

Induced pluripotent stem (iPS) cells, which are generated from somatic cells by transducing four genes, are expected to have broad application to regenerative medicine. Although establishment of an efficient gene transfer system for iPS cells is considered to be essential for differentiating them into functional cells, the detailed transduction characteristics of iPS cells have not been examined. By using an adenovirus (Ad) vector containing the cytomegalovirus enhancer/beta-actin (CA) promoters, we have developed an efficient transduction system for mouse mesenchymal stem cells and embryonic stem (ES) cells. Also, we applied our transduction system to mouse iPS cells and investigated whether efficient differentiation could be achieved by Ad vector-mediated transduction of a functional gene. As in the case of ES cells, the Ad vector could efficiently transduce transgenes into mouse iPS cells. We found that the CA promoter had potent transduction ability in iPS cells. Moreover, exogenous expression of a PPARγ gene or a Runx2 gene into mouse iPS cells by an optimized Ad vector enhanced adipocyte or osteoblast differentiation, respectively. These results suggest that Ad vector-mediated transient transduction is sufficient to promote cellular differentiation and that our transduction methods would be useful for therapeutic applications based on iPS cells.

Key words——regenerative medicine; induced pluripotent stem (iPS) cell; adenovirus vector; mesenchymal stem cell; embryonic stem (ES) cell

1. はじめに

幹細胞（stem cells）は自己複製能と分化多能性という大きく2つの特徴を有する細胞であり，目的の細胞へ分化させることにより創薬や再生医療への応用が期待されている．再生医療への応用が期待されている幹細胞には，造血幹細胞，神経幹細胞，間葉系幹細胞，ES（embryonic stem）細胞，iPS（induced pluripotent stem）細胞などがある．このうち，ES細胞は受精卵（胚）から樹立され，iPS細胞は体細胞に4種の遺伝子（Oct-3/4m Sox2, Klf4, c-Myc）を導入することにより作製される．しかしながら，ES細胞やiPS細胞を直接生体に移植するには困難な場合も多く，マウス生体に投与するとランダムに分化しテラトーマ（奇形腫）を形成する．したがって，治療目的には幹細胞を *in vitro* で目的の細胞に分化させた後生体に移植することが望ましいと考えられる．幹細胞を骨，心筋，脂肪，血液などの目的の細胞に分化させるには，培養液に特定のサイトカインや増殖因子等の液性因子を加える方法がとられているが分化効率は十分ではない．そこで，われわれは各種幹細胞に機能遺伝子を導入することにより効率よく分化させることができないかと考え研究を進めている．一般に，幹細胞は遺伝子導入が困難であり，リポフェクション法やレトロウイルスベクター系など通常用いられる方法では十分な導入効率が得られない．われわれは高効率かつ一過性に目的遺伝子を発現させることができるアデノウイルス（Ad）ベクターを用いて機能遺伝子を導入

[a]独立行政法人医薬基盤研究所幹細胞制御プロジェクト（〒567-0085 大阪府茨木市彩都あさぎ7-6-8），[b]大阪大学大学院薬学研究科医薬基盤科学分野，[c]同分子生物学分野（〒565-0871 大阪府吹田市山田丘1-6）
*e-mail: kawabata@nibio.go.jp

本総説は，日本薬学会第130年会シンポジウムS19で発表したものを中心に記述したものである．

することにより，幹細胞の分化誘導効率を向上させることを目指した．

2. 間葉系幹細胞への遺伝子導入

間葉系幹細胞は骨髄由来のストローマ細胞であり，骨，軟骨，脂肪，心筋系列などの中胚葉系細胞に分化することができ，未分化状態で細胞を容易に増殖させることができる．[1] また，最近では，間葉系幹細胞は神経細胞，肝細胞，インスリン産生細胞などの外胚葉や内胚葉系の細胞へも分化するという報告もあり，再生医療や組織工学への応用が強く期待されている．間葉系幹細胞の分化を制御する手段の1つとして，細胞分化に関与する遺伝子を導入することが挙げられる．Ad ベクターを用いた間葉系幹細胞への遺伝子導入も試みられてきたが，間葉系幹細胞は Ad 受容体 CAR（coxsackievirus and adenovirus receptor）を発現していないためにその導入効率は極めて低く，遺伝子導入には高タイターのベクターを必要としていた．[2,3] われわれは，独自に開発した種々のファイバー改変型 Ad ベクターを用いて間葉系幹細胞にレポーター遺伝子を導入し，その発現効率を比較検討した．[4,5] 間葉系幹細胞を多く含有する画分であるマウス骨髄ストローマ細胞を用いて遺伝子導入効率を測定した結果，間葉系幹細胞にはファイバーにポリリジン残基を挿入した K7 型ベクターが最も適しており，従来型ベクターの 100 倍以上の遺伝子導入効率を示すことが明らかとなった［Figs. 1 (A) and (B)］．RGD 型ベクターは従来型ベクターに比較し 10 倍程度の導入効率を示した．また，種々のプロモーターを用いて比較検討したところ，CA プロモーターが最適であった［Fig. 1 (C)］．したがって，間葉系幹細胞には CA プロモーターを有する K7 型 Ad ベクターを用いることにより最も高効率に遺伝子導入できることが明らかとなった．間葉系幹細胞は様々な系列の細胞に分化するというだけではなく，担がんマウスに投与された場合には腫瘍に集積する性質を有している．[6] し

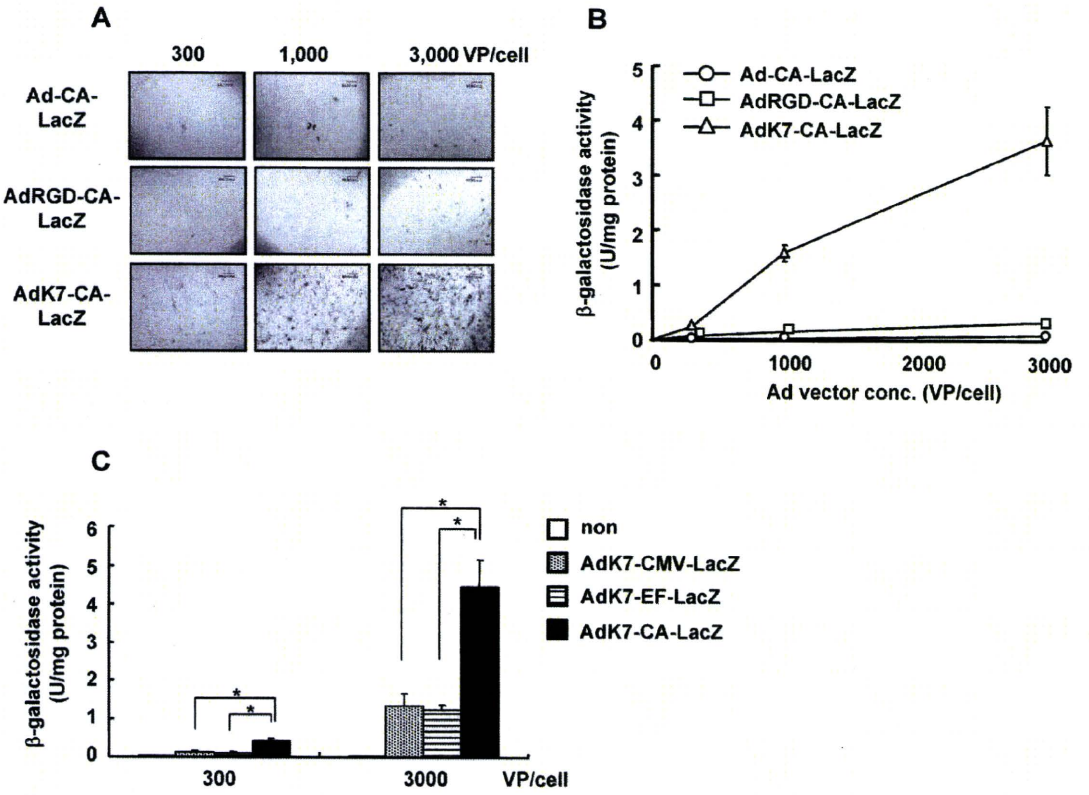

Fig. 1. Gene Transduction Efficiency in Mouse Primary BMSCs by Various Types of Ad Vectors

Mouse primary BMSCs were transduced with the indicated doses of LacZ-expressing Ad vectors for 1.5 h. Two days later, (A) X-gal staining and (B) luminescence assay were carried out. Similar results of X-gal staining were obtained in three independent experiments. Scale bar indicates 200 μm. (C) Optimization of promoter activity in BMSCs using LacZ-expressing AdK7. BMSCs were transduced with each Ad vector at 300 or 3000 VP/cell, and LacZ expression in the cells was measured. The data (B and C) are expressed as mean±S.D. (n=3). *p<0.01.

たがって，間葉系幹細胞は分化させた細胞自身を治療に利用するだけでなく，抗腫瘍性サイトカイン等を発現する間葉系幹細胞をがんに対する細胞治療薬として利用できる可能性があり，現在検討している．

3. 間葉系幹細胞の分化誘導

間葉系幹細胞への遺伝子導入にはCAプロモーターを有したK7型Adベクターが最適であることが明らかとなったので，次に本ベクターを用いて機能遺伝子を導入し分化誘導効率を向上させることを試みた．Runx2はRuntファミリーに属する転写因子であり，Runx2遺伝子欠損マウスは骨芽細胞分化が初期で停止し骨形成が欠損することが知られている．[7] そこで，Runx2遺伝子をマウス骨髄ストローマ細胞に導入した結果，従来の分化誘導法と比較しアルカリホスファターゼ活性の上昇及びカルシウムの沈着がみとめられ，著明に骨芽細胞への分化誘導効率が促進されることが明らかとなった［Figs. 2(A) and (B)］．また，それに伴い，タイプIコラーゲン，オステリクス，オステオカルシン等の骨芽細胞マーカー遺伝子の発現も上昇した［Fig. 2(C)］．さらに，このようにして分化誘導した骨芽細胞をマウスに移植したところ，Fig. 3に示すように異所性の骨形成がみとめられ，*in vivo*においても機能を有していることが示された．以上より，本ベクターは*in vitro*及び*in vivo*において間葉系細胞を効率よく骨芽細胞へ分化誘導するのに適したベクターであることが示された．

4. マウスES細胞及びマウスiPS細胞への遺伝子導入

ES細胞は胚盤胞内部細胞塊由来の細胞であり，無限に増殖するとともにすべての機能細胞に分化する性質を有する．一方，iPS細胞は体細胞に4種の遺伝子（Oct-3/4, c-myc, Sox2, Klf4）を同時に導入することにより得られる人工多能性幹細胞であり，倫理的な問題を回避できることから再生医療への応用が大きく期待されている．[8] しかしながら，これら幹細胞の分化を自由に制御する技術はいまだ確立されておらず，その原因の1つとして効率よい遺伝子導入法が確立されていないことが挙げられる．これまで，ES細胞に対しては，プラスミドDNAを用いたエレクトポレーション法（プラスミドDNAを電気的刺激により細胞内に導入し，染色体にわずかに目的遺伝子と薬剤耐性遺伝子が組み込まれた細胞を薬剤で選択する方法），[9] レトロウイルスベクター，[10] レンチウイルスベクター，[11] ポリオーマウイルスの複製機構を利用したスーパートランスフェクション法（ポリオーマウイルスの複製起点を含んだプラスミドDNAがマウスES細胞ではエピゾーマルに増幅できる性質を利用した方法）[12] などが外来遺伝子導入法として用いられてきた．しかしながら，これらは半永久的に導入遺伝子を発現し続ける方法であり，ES細胞やiPS細胞の分化制御，特に医療目的などの細胞分化後には発現を停止させたい場合には好ましくない．Adベクターは導入遺伝子が宿主染色体へ組込まれることなく，染色体外にエピゾームとして存在することから（増幅しない），遺伝子発現が一過性であり，ES細胞やiPS細胞を目的の機能細胞に分化させた後は導入遺伝子の発現が消失するものと期待される．そこで，筆者らは，マウスES細胞及びiPS細胞に最も適したAdベクターによる遺伝子導入法の確立を試みた．その結果，マウスES細胞やiPS細胞はAd受容体CARを高発現しており，従来型アデノウイルスベクターが最適であることが明らかとなった．[13,14] また，RSV, CMV, CA（β-actin promoter/CMV enhancer），EF-1αの4種のプロモーターを用いて検討した結果，ES細胞及びiPS細胞ではCA及びEF-1αプロモーターを用いた場合にのみ遺伝子発現がみられ，RSVやCMVプロモーターはほとんど機能しなかった［Fig. 4(A)］．これまでAdベクターはES細胞への遺伝子導入には不適と考えられてきたが，これは多くの場合，最も一般的に用いられているCMVプロモーターを用いて検討されてきたためであり，ウイルスの細胞へのエントリー自体には問題がないことが示された．ただし，CAプロモーターを用いた場合にはES細胞のみならずその支持細胞（フィーダー細胞）である胚繊維芽細胞にも遺伝子発現がみられたのに対し，EF-1αプロモーターを用いた場合にはほぼES細胞特異的に遺伝子発現可能であった．これは，EF-1αプロモーターの活性が胚繊維芽細胞に比べES細胞において相対的に高いことが原因と考えられる．したがって，目的により両プロモーターを使い分けることによって，再生医療への幅広い応用が期待できる．

Adベクターを導入することによりES細胞やiPS細胞が有する本来の性質が失われると再生医療

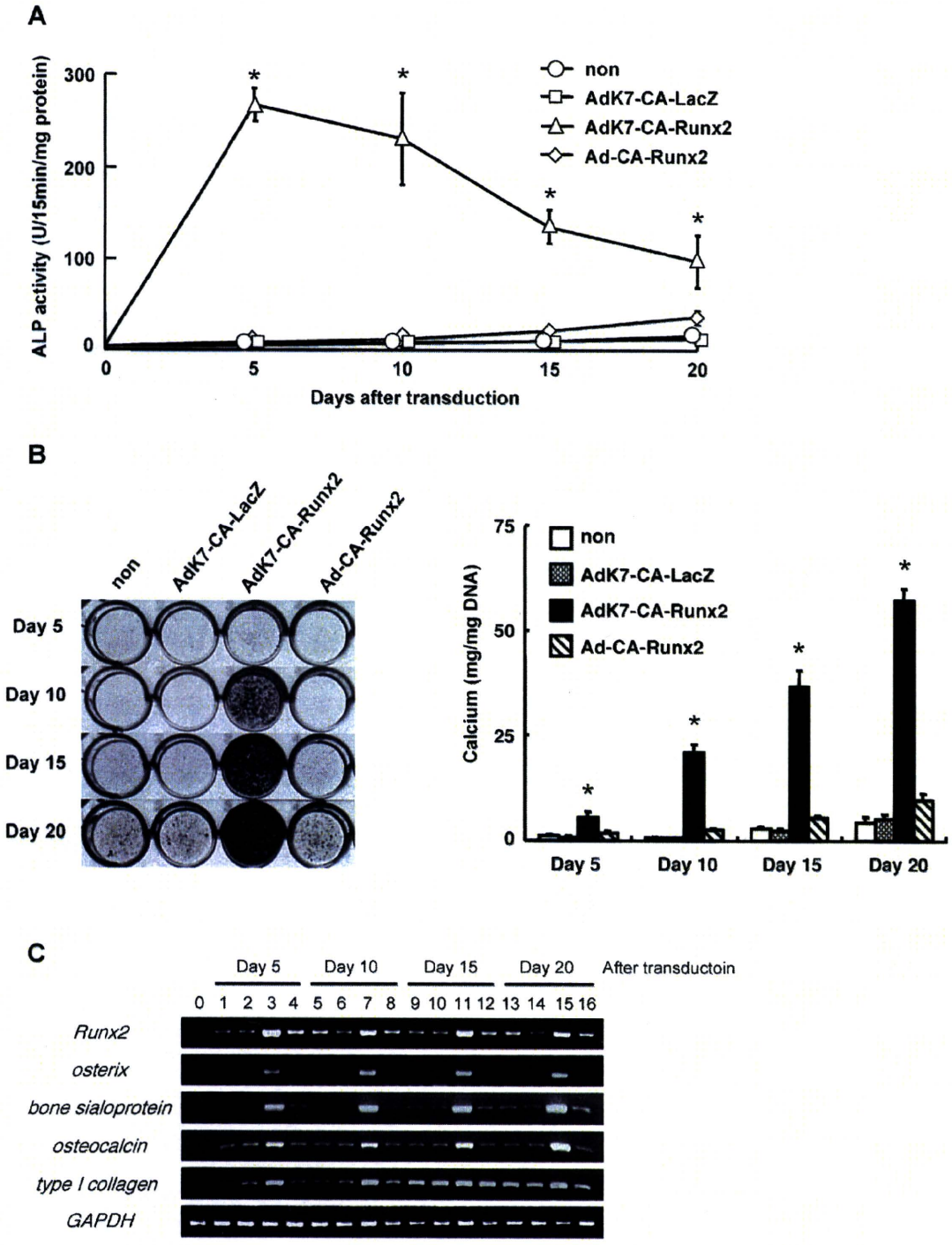

Fig. 2. Promotion of *in Vitro* Osteoblastic Differentiation in BMSC Transduced with AdK7-CA-Runx2

BMSCs were transduced with each Ad vector at 3000 VP/cell for 1.5 h, and were cultured for the indicated number of days. (A) Alkaline phosphatase activity, (B, left) matrix minerarization, and (B, right) calcium deposition in the cells was determined as described in Materials and Methods. The data are expressed as mean±S.D. (n=3). *p<0.01 as compared with non-, AdK7-CA-LacZ-, or Ad-CA-Runx2-transduced cells. (C) RT-PCR was carried out using primers for Runx2, osterix, bone sialoprotein, osteocalcin, collagen type I, and GAPDH. Lane 0: non-treated BMSCs; lanes 1, 5, 9, and 13: BMSCs with osteogenic supplements (OS); lanes 2, 6, 10, and 14: BMSCs with OS plus AdK7-CA-LacZ; lanes 3, 7, 11, and 15: BMSCs with OS plus AdK7-CA-Runx2; lanes 4, 8, 12, and 16: BMSCs with OS plus Ad-CA-Runx2.

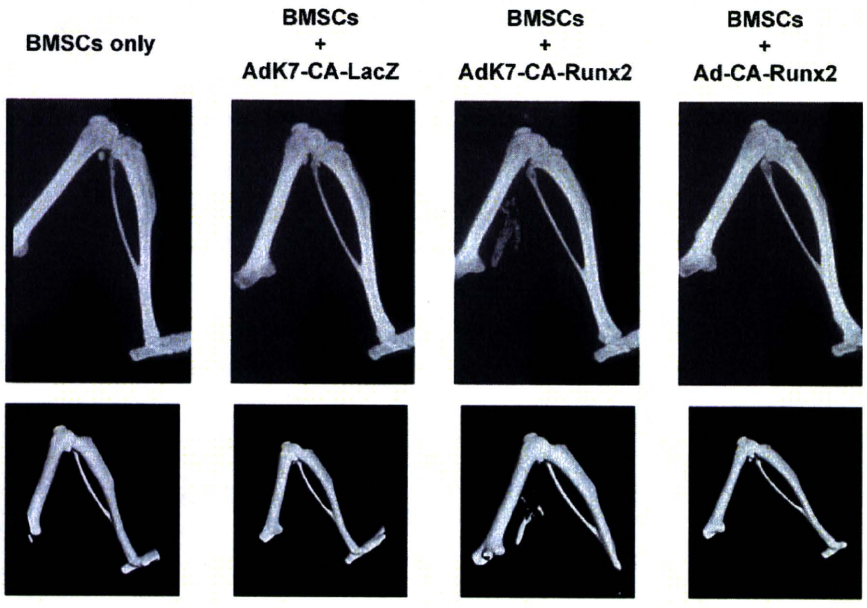

Fig. 3. *In vivo* Ectopic Bone Formation of Mouse BMSCs by AdK7-mediated Runx2 Gene Transduction

BMSCs were transduced with indicated Ad vectors at 3000 VP/cell for 1.5 h. On the following day, cells (2×10^6 cells) were suspended in PBS and injected into the hind limb biceps muscle of nude mice. Four weeks later, bone formation was analyzed by the microCT system. Similar results were obtained in two independent experiments. Upper, X-ray images; lower, 3D reconstitution images.

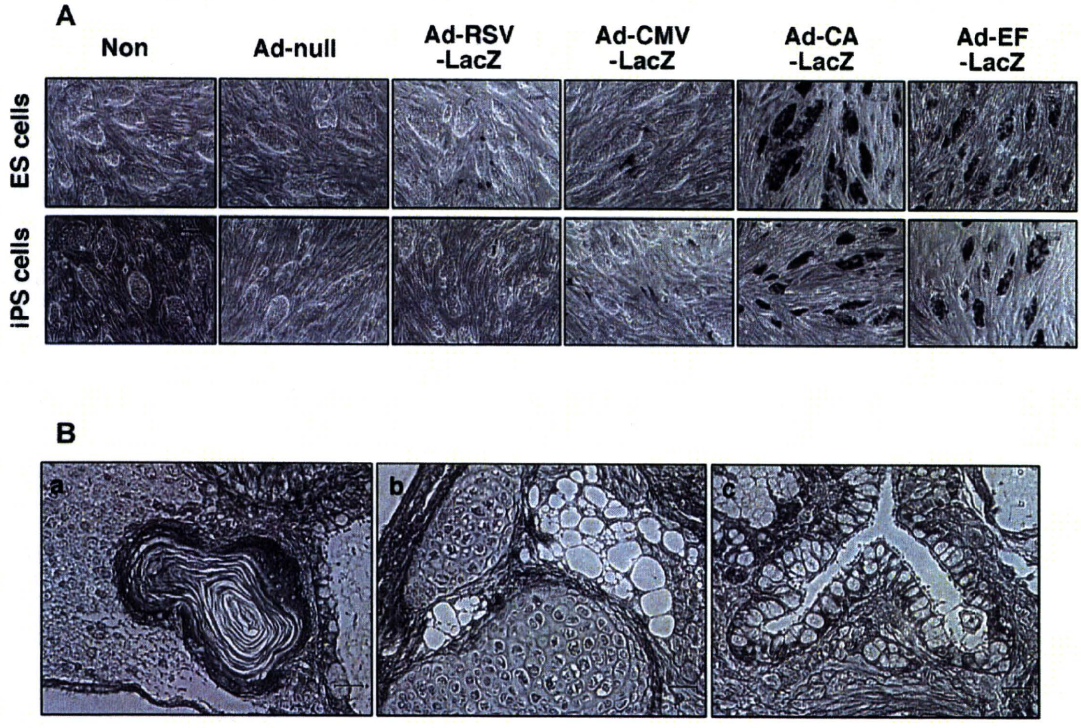

Fig. 4. Efficient Transgene Expression in Mouse iPS Cells by Using an Ad Vector Containing the CA and the EF-1α Promoter

(A) Mouse ES cells or iPS cells were transduced with LacZ-expressing Ad vector at 3000 VP/cell. On the following day, X-gal staining was carried out. Similar results of X-gal staining were obtained in three independent experiments. (B) Paraffin sections of the teratomas derived from Ad-CA-mCherry-transduced iPS cells were prepared, and sections were stained with hematoxylin and eosin. a, ectoderm (epidermis); b, mesoderm (cartilage and adipocyte); c, endoderm (gut epithelium).